

ARTICLE

# Perlecan regulates pericyte dynamics in the maintenance and repair of the blood–brain barrier

Kuniyuki Nakamura<sup>1,2</sup>, Tomoko Ikeuchi<sup>1</sup>, Kazuki Nara<sup>1,3</sup>, Craig S. Rhodes<sup>1</sup>, Peipei Zhang<sup>1</sup>, Yuta Chiba<sup>1</sup>, Saiko Kazuno<sup>4</sup>, Yoshiki Miura<sup>4</sup>, Tetsuro Ago<sup>2</sup>, Eri Arikawa-Hirasawa<sup>5</sup>, Yoh-suke Mukouyama<sup>6</sup>, and Yoshihiko Yamada<sup>1</sup>

Ischemic stroke causes blood–brain barrier (BBB) breakdown due to significant damage to the integrity of BBB components. Recent studies have highlighted the importance of pericytes in the repair process of BBB functions triggered by PDGFR $\beta$  up-regulation. Here, we show that perlecan, a major heparan sulfate proteoglycan of basement membranes, aids in BBB maintenance and repair through pericyte interactions. Using a transient middle cerebral artery occlusion model, we found larger infarct volumes and more BBB leakage in conditional perlecan (*Hspg2*<sup>−/−</sup>-TG) mice than in control mice. Control mice showed increased numbers of pericytes in the ischemic lesion, whereas *Hspg2*<sup>−/−</sup>-TG mice did not. At the mechanistic level, pericytes attached to recombinant perlecan C-terminal domain V (perlecan DV, endorepellin). Perlecan DV enhanced the PDGF-BB-induced phosphorylation of PDGFR $\beta$ , SHP-2, and FAK partially through integrin  $\alpha 5 \beta 1$  and promoted pericyte migration. Perlecan therefore appears to regulate pericyte recruitment through the cooperative functioning of PDGFR $\beta$  and integrin  $\alpha 5 \beta 1$  to support BBB maintenance and repair following ischemic stroke.

## Introduction

The blood–brain barrier (BBB) is a highly selective permeability barrier that protects the central nervous system from a constantly changing environment in the blood, as well as from blood-borne pathogens and toxins. Ischemic stroke causes a loss of integrity of the BBB components, which leads to breakdown of the BBB and subsequent enlargement of the infarction, brain edema, and hemorrhagic transformation (Baeten and Akassoglou, 2011). The BBB consists mainly of specialized brain endothelial cells that are intimately connected by tight junctions and covered by basement membranes (BMs), pericytes that extend multiple cytoplasmic processes covering endothelial cells, and the end-feet of astrocytes. Degradation of the BM is known to trigger the disruption of the BBB (Del Zoppo et al., 2006; Baeten and Akassoglou, 2011), but the manner in which each BM component responds to ischemic stroke is not yet fully understood.

All BMs and cartilage contain perlecan, a large multidomain heparan sulfate proteoglycan (HSPG) of the ECM (Arikawa-Hirasawa et al., 1999). Perlecan mediates numerous cellular activities and regulates tissue homeostasis by interacting with

many other ECM proteins, growth factors, and receptors (Kerever et al., 2014; Lord et al., 2014). As several of these ECM components have various biological activities that depend on their C-terminus fragments, the perlecan C-terminal domain V (perlecan DV, endorepellin) triggers anti-angiogenic activity in endothelial cells through the dual binding of integrin  $\alpha 2 \beta 1$  and VEGFR2 (Mongiat et al., 2003; Bix et al., 2004; Woodall et al., 2008; Goyal et al., 2011). Recent reports have indicated that perlecan DV also plays pro-angiogenic and neuroprotective roles in ischemic stroke through enhanced production of VEGF in brain endothelial cells that express integrin  $\alpha 5 \beta 1$  rather than integrin  $\alpha 2 \beta 1$  (Lee et al., 2011; Clarke et al., 2012). Despite the importance of perlecan DV in endothelial cell behaviors, any effect on pericytes remains to be established.

Conventional Perlecan knockout (KO) mice (i.e., *Hspg2*<sup>−/−</sup>) die just after birth due to respiratory failure caused by their cartilage defects (Arikawa-Hirasawa et al., 1999; Costell et al., 1999). We have been able to avoid this lethality by creating conditional Perlecan-deficient (*Hspg2*<sup>−/−</sup>-TG [Perlecan KO]) mice that express the Perlecan transgene only in cartilage; this was done

<sup>1</sup>Molecular Biology Section, National Institute of Dental and Craniofacial Research, National Institutes of Health, Bethesda, MD; <sup>2</sup>Department of Medicine and Clinical Science, Graduate School of Medical Sciences, Kyushu University, Fukuoka, Japan; <sup>3</sup>Tohoku University School of Medicine, Sendai, Japan; <sup>4</sup>Laboratory of Proteomics and Biomolecular Science, Research Support Center, Juntendo University Graduate School of Medicine, Tokyo, Japan; <sup>5</sup>Research Institute for Diseases of Old Age, Juntendo University Graduate School of Medicine, Tokyo, Japan; <sup>6</sup>Laboratory of Stem Cell and Neuro-Vascular Biology, Cell and Developmental Biology Center, National Heart, Lung, and Blood Institute, National Institutes of Health, Bethesda, MD.

Correspondence to Kuniyuki Nakamura: [kunakamu@intmed2.med.kyushu-u.ac.jp](mailto:kunakamu@intmed2.med.kyushu-u.ac.jp); Yoshihiko Yamada: [yyamada@dir.nidcr.nih.gov](mailto:yyamada@dir.nidcr.nih.gov).

This is a work of the U.S. Government and is not subject to copyright protection in the United States. Foreign copyrights may apply. This article is distributed under the terms of an Attribution–Noncommercial–Share Alike–No Mirror Sites license for the first six months after the publication date (see <http://www.rupress.org/terms/>). After six months it is available under a Creative Commons License (Attribution–Noncommercial–Share Alike 4.0 International license, as described at <https://creativecommons.org/licenses/by-nc-sa/4.0/>).

using the *Col2a1* promoter and enhancer (Xu et al., 2010). These mice have been used to uncover roles for perlecan in muscle homeostasis (Xu et al., 2010; Ning et al., 2015), self-renewal of neural stem cells and neurogenesis (Kerever et al., 2014), vascularization during endochondral bone formation (Ishijima et al., 2012), and endothelial-derived relaxing function (Nonaka et al., 2015).

Recent studies have demonstrated that the process of BBB repair involves pericyte recruitment, which is triggered by the up-regulation of platelet-derived growth factor receptor  $\beta$  (PDGFR $\beta$ ) in peri-infarct areas (Arimura et al., 2012; Makiyama et al., 2015; Nakamura et al., 2016). PDGFR $\beta$  is a key molecule that drives pericyte migration, and PDGFR $\beta$  signaling is required for pericyte recruitment toward endothelial tubes in the developmental stage of vascular and neural tissues (Lindahl et al., 1997; Hellstrom et al., 2001). Following ischemic stroke, up-regulation of PDGFR $\beta$  is essential for maintenance of the BBB and the repair process in the infarct areas (Arimura et al., 2012; Shen et al., 2012; Makiyama et al., 2015; Nakamura et al., 2016). However, the identity and mechanism of action of the actual ECM components that modulate PDGFR $\beta$  signaling and regulate pericyte behaviors in the microenvironment after ischemic stroke remain unclear.

In the present study, we show that perlecan is an important ECM component in the BBB, as it plays a protective role against ischemic BBB disruption. Perlecan maintains BBB integrity and enhances pericyte migration through a cooperative function of PDGFR $\beta$  and integrin  $\alpha 5 \beta 1$  signaling, thereby contributing to the repair process of the BBB following ischemic stroke.

## Results

### Perlecan is essential for BBB maintenance after ischemic stroke

We identified the function of perlecan in the BBB by first examining the expression of perlecan in the adult brain of wild-type mice. Perlecan was colocalized with the tomato lectin-positive brain endothelial cells and was found adjacent to PDGFR $\beta$ -positive brain pericytes (Fig. 1 A). Compared with brain pericytes, brain endothelial cells highly expressed HSPG2 (Perlecan) mRNA in vitro (Fig. 1 B), suggesting the presence of endothelial cell-derived perlecan in the BMs between the endothelial cells and pericytes and that perlecan may represent a major ECM component of the BBB.

The conditional Perlecan-deficient (*Hspg2*<sup>-/-</sup>-TG, Perlecan KO) mice had no detectable expression of perlecan in the brain vasculature (Fig. 1 C, TG and control vs. Perlecan KO). Under normal conditions, the brain vasculature of the Perlecan KO mice showed normal morphology, including normal pericyte coverage (Fig. S1, A and B). The expression of the tight junction proteins, Claudin-5 and ZO-1, was also not significantly changed in the Perlecan KO mice (Fig. S1, C–F). Injection of Evans Blue as an exogenous tracer revealed no extravasation (not depicted), suggesting that Perlecan deficiency does not affect the BBB structure and function under normal conditions.

We next evaluated the function of perlecan after ischemic stroke using Perlecan KO mice subjected to 60-min middle

cerebral artery occlusion (MCAO) as a stroke model. Staining with 2,3,5-triphenyltetrazolium chloride (TTC) revealed a larger infarct size in the Perlecan KO mice than in control mice at postsurgery day (PSD) 2 (Fig. 1, D and E; and Fig. S2 A). BBB leakage, evaluated by Evans Blue extravasation, was greater in Perlecan KO mice than in control mice at PSD 2, which is a peak time point for BBB disruption (Fig. 1, F and G). The extravasation of fibrinogen, an endogenous marker of BBB leakage, was also greater in Perlecan KO mice than in control mice (Fig. 1, H and I). The loss of the tight junction proteins, Claudin-5 and ZO-1, in the infarct areas was also greater in Perlecan KO mice than in control mice (Fig. 1, J and K). These results indicate that Perlecan deficiency enhances BBB disruption following ischemic stroke.

### Perlecan is necessary for pericyte accumulation after ischemic stroke

Our previous studies demonstrated that PDGFR $\beta$  expression is gradually up-regulated in pericytes in peri-infarct areas over the initial 3 d following ischemic stroke and that maintenance and repair of the BBB might require the PDGFR $\beta$  signaling pathway (Arimura et al., 2012; Makiyama et al., 2015; Nakamura et al., 2016). In agreement with these previous findings, the expression of pericyte markers, including CD13, PDGFR $\beta$ , desmin, and NG2, was up-regulated in the ischemic lesion of control mice at PSD 3 after MCAO, as indicated by immunofluorescence analysis of brain sections (Fig. 2, A–G; and Fig. S2 B). However, this up-regulation of pericyte markers was attenuated in the Perlecan KO mice (Fig. 2, A–H). The Perlecan KO mice appeared to have a worse neurological deficit, a lower survival rate, increased hemorrhagic transformation, and greater weight loss after MCAO compared with control mice (Fig. S2, C–F). These results suggest that perlecan may contribute to pericyte accumulation and the subsequent neurological deficits observed following ischemic stroke.

### Perlecan expression is up-regulated after ischemic stroke

Previous studies suggest that BM degradation and BBB breakdown occur after ischemic stroke (Baeten and Akassoglou, 2011). In control mice, however, perlecan expression at PSD 3 was significantly increased in the ischemic lesion compared with the contralateral hemisphere (Fig. 3, A–C). Up-regulation of the endothelial cell marker CD31 was accompanied by up-regulation of perlecan in the ischemic lesion (Fig. 3 A). Similarly, expression of the BM proteins such as laminin  $\alpha 5$  and collagen type IV was also increased in the ischemic lesion (Fig. S3, A and B). However, there was no significant difference in the expression of these BM proteins between control and Perlecan KO mice.

Integrins are heterodimeric transmembrane receptors for ECM proteins and have a known involvement in the biological activities of those proteins (Hood and Chersesh, 2002; Iozzo, 2005). We addressed a potential influence of perlecan on integrin-mediated pericyte behaviors by examining integrin expression in cultured brain pericytes, as well as in brain endothelial cells and in human umbilical vein endothelial cells. Both brain pericytes and brain endothelial cells strongly expressed ITGA5 (integrin  $\alpha 5$ ) and ITGB1 ( $\beta 1$ ; Fig. 3 D and Table 1), and in vitro exposure of pericytes to hypoxia at 1% O<sub>2</sub>

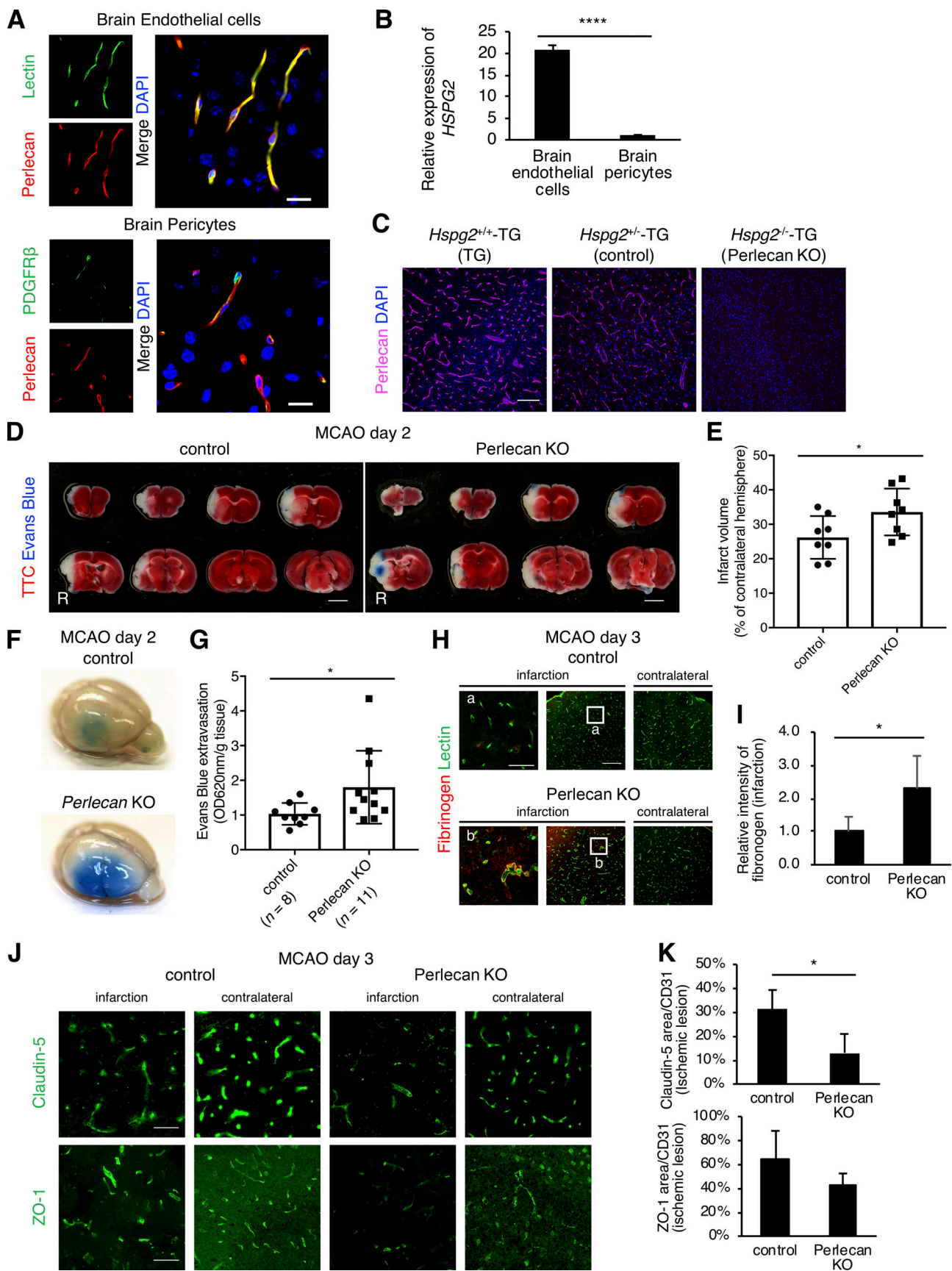


Figure 1. **The BBB is strongly disrupted after ischemic stroke in Perlecan KO mice.** (A) The expression of perlecan (red) colocalized with lectin-positive brain endothelial cells (green, upper panels) and was found adjacent to PDGFR $\beta$ -positive brain pericytes (green, lower panels) in a brain section of wild-type



mice. Scale bar = 20  $\mu\text{m}$ . **(B)** Quantitative PCR for *HSPG2* (Perlecan) in cultured brain endothelial cells and pericytes. Values are mean  $\pm$  SD;  $n = 4$ ; \*\*\*\*,  $P < 0.0001$ , unpaired  $t$  test. **(C)** Perlecan was expressed in brain vasculature in *Hspg2<sup>+/+</sup>*-TG (TG) and *Hspg2<sup>-/-</sup>*-TG (control) mice, but not in conditional perlecan-deficient (*Hspg2<sup>-/-</sup>*-TG [Perlecan KO]) mice. Scale bar = 100  $\mu\text{m}$ . **(D and E)** Representative images of TTC staining (D) at PSD 2 after MCAO in control and Perlecan KO mice and the quantified infarct volume (E). Evans Blue was injected into these mice to show the BBB leakage (Evans Blue extravasation). Scale bar = 3 mm. The infarction volume was significantly greater in Perlecan KO mice than in control mice. Values are mean  $\pm$  SD;  $n = 8$  mice per group; \*,  $P < 0.05$ , unpaired  $t$  test. **(F and G)** Representative images of Evans Blue extravasation at PSD 2 after MCAO in control and Perlecan KO mice (F). Quantification of Evans Blue extracted from ipsilateral hemispheres at PSD 2 (G) showed more leakage of the dye in Perlecan KO mice than in control mice. Values are mean  $\pm$  SD;  $n = 8$ –11 mice per group; \*,  $P < 0.05$ , unpaired  $t$  test. **(H and I)** Representative images of fibrinogen extravasation at PSD 3 after MCAO in control and Perlecan KO mice. Left panels show a higher magnification of the indicated lesion in the infarction. Scale bar = 40  $\mu\text{m}$  (left panels) or 150  $\mu\text{m}$  (middle and right panels). Quantification of fibrinogen intensity (I) showed more leakage in Perlecan KO mice than in control mice. Values are mean  $\pm$  SD;  $n = 5$  mice per group; \*,  $P < 0.05$ , unpaired  $t$  test. **(J and K)** Representative images of the immunostaining for Claudin-5 (upper panels) and ZO-1 (lower panels) at PSD 3 after MCAO in the brain cortex of control and Perlecan KO mice (J). Scale bar = 50  $\mu\text{m}$ . Claudin-5-positive and ZO-1-positive areas were quantified and standardized by CD31-positive areas in the ischemic lesions of control and Perlecan KO mice (K). Values are mean  $\pm$  SD;  $n = 4$  mice per group; \*,  $P < 0.05$ , unpaired  $t$  test.

up-regulated these expressions (Table 1). Moreover, integrin  $\alpha 5$  expression was significantly up-regulated in the ischemic lesions of both control and Perlecan KO mice following MCAO (Fig. 3, E and F). High-resolution triple immunofluorescence imaging of brain microvessels revealed that the expression of integrin  $\alpha 5$  was up-regulated in both endothelial cells and pericytes in the ischemic lesions (Figs. 3 G and S3 C). These results indicate that ischemic stroke induces the up-regulation of perlecan and its potential receptor, integrin  $\alpha 5\beta 1$ .

#### Perlecan DV attaches to pericytes and promotes PDGFR $\beta$ signaling through integrin $\alpha 5\beta 1$

Perlecan consists of a core protein with three long attached chains of glycosaminoglycan (heparan sulfate; Fig. 4 A; Noonan et al., 1991). The biological activities of perlecan are known to depend on the C-terminus fragment of the core protein, DV (endorepellin; Iozzo, 2005), which contains three globular domains that show homology with laminin G module and are each separated by EGF-like repeats. To examine the biological activities of perlecan DV in pericyte behaviors, we developed recombinant FLAG-tagged perlecan DV (Fig. S3 D). Both purified full-length perlecan and perlecan DV showed a substantial attachment to human brain pericytes in the 30-min adhesion assay (Fig. 4 B). Function-blocking antibodies against integrin  $\alpha 5$  (mAb16) and  $\beta 1$  (mAb13) inhibited the adhesion of perlecan DV to pericytes, but mAb16 treatment did not inhibit the adhesion of full-length perlecan (Fig. 4 B). Similarly, perlecan DV showed a substantial attachment to brain endothelial cells, and this adhesion was inhibited by mAb16 (Fig. S3 E). Taken together, these results suggested that the adhesion of perlecan DV to both pericytes and endothelial cells occurs through integrin  $\alpha 5$ , and the perlecan-integrin  $\alpha 5$ -mediated adhesion may contribute to the integrity of these vascular components.

To examine the direct binding of perlecan DV to integrin  $\alpha 5\beta 1$ , we performed a solid-phase binding assay. The binding affinity of immobilized perlecan DV to integrin  $\alpha 5\beta 1$  was significant, albeit to a lesser level (Fig. 4 C). Therefore, we further investigated the binding of perlecan DV to integrin  $\alpha 5\beta 1$  using a surface plasmon resonance (SPR) assay that allows us to detect these interacting proteins without labeling them. The SPR assays showed an association of perlecan DV with integrin  $\alpha 5\beta 1$  (Fig. S3 F), whereas fibronectin bound to integrin  $\alpha 5\beta 1$  with high affinity (Figs. 4 C and S3 G).

We should note that the sensorgram of the perlecan DV-integrin  $\alpha 5\beta 1$  did not appear a typical isotherm. Combined, these data suggest that the binding of perlecan DV to integrin  $\alpha 5\beta 1$  was observed, but with such a weak interaction, we could not obtain unequivocal evidence for a direct interaction.

We next examined a potential influence of perlecan on the PDGF-BB/PDGFR $\beta$  signaling pathway, which is an important pathway for pericyte recruitment (Quaegebeur et al., 2011; Winkler et al., 2011). Results from solid-phase binding assays clearly demonstrated a direct association of PDGF-BB, but not its receptor PDGFR $\beta$ , with both immobilized full-length perlecan and perlecan DV (Fig. 4 D). These findings suggest that the interaction between perlecan and PDGF-BB may enhance PDGF-BB-mediated pericyte recruitment. Interestingly, the mechanism underlying the interaction between perlecan and PDGF-BB/PDGFR $\beta$  signaling appears to differ from the one underlying the interaction between perlecan and basic fibroblast growth factor (bFGF)/fibroblast growth factor receptor (FGFR) signaling, as previous studies have shown a direct interaction of perlecan with both bFGF and FGFR (Ishijima et al., 2012).

Further examination of the effect of perlecan DV on the PDGFR $\beta$  signaling pathway in pericytes revealed an enhancement of the PDGF-BB-induced PDGFR $\beta$  phosphorylation when pericytes were cultured on the perlecan DV-coated plates (Fig. 4 E). These results suggest a mechanism by which perlecan DV could amplify the PDGF-BB/PDGFR $\beta$  signaling through the binding of perlecan DV with PDGF-BB. We next examined whether integrin  $\alpha 5$  influences the PDGFR $\beta$  signaling pathway in pericytes by analyzing the activity of Src homology 2 domain-containing phosphatase 2 (SHP-2) and FAK, which are two common downstream molecules of PDGFR $\beta$  and integrin (Tallquist et al., 2003; Huttenlocher and Horwitz, 2011; Sweeney et al., 2016). Interestingly, perlecan DV enhanced SHP-2 phosphorylation in the presence of PDGF-BB (Fig. 4 E). Similarly, perlecan DV enhanced FAK phosphorylation (Fig. 4 E). The phosphorylation of both SHP-2 and FAK were inhibited by the integrin  $\alpha 5$  blocking antibody mAb16, whereas mAb16 did not alter the phosphorylation of PDGFR $\beta$  (Fig. 4 F). These results suggest that integrin  $\alpha 5$  may be involved in perlecan DV-mediated enhancement of SHP-2 and FAK phosphorylation, but it may not affect the binding of perlecan DV with PDGF-BB and perlecan DV-mediated enhancement of PDGF-BB-induced PDGFR $\beta$  phosphorylation. Perlecan DV influences the activation

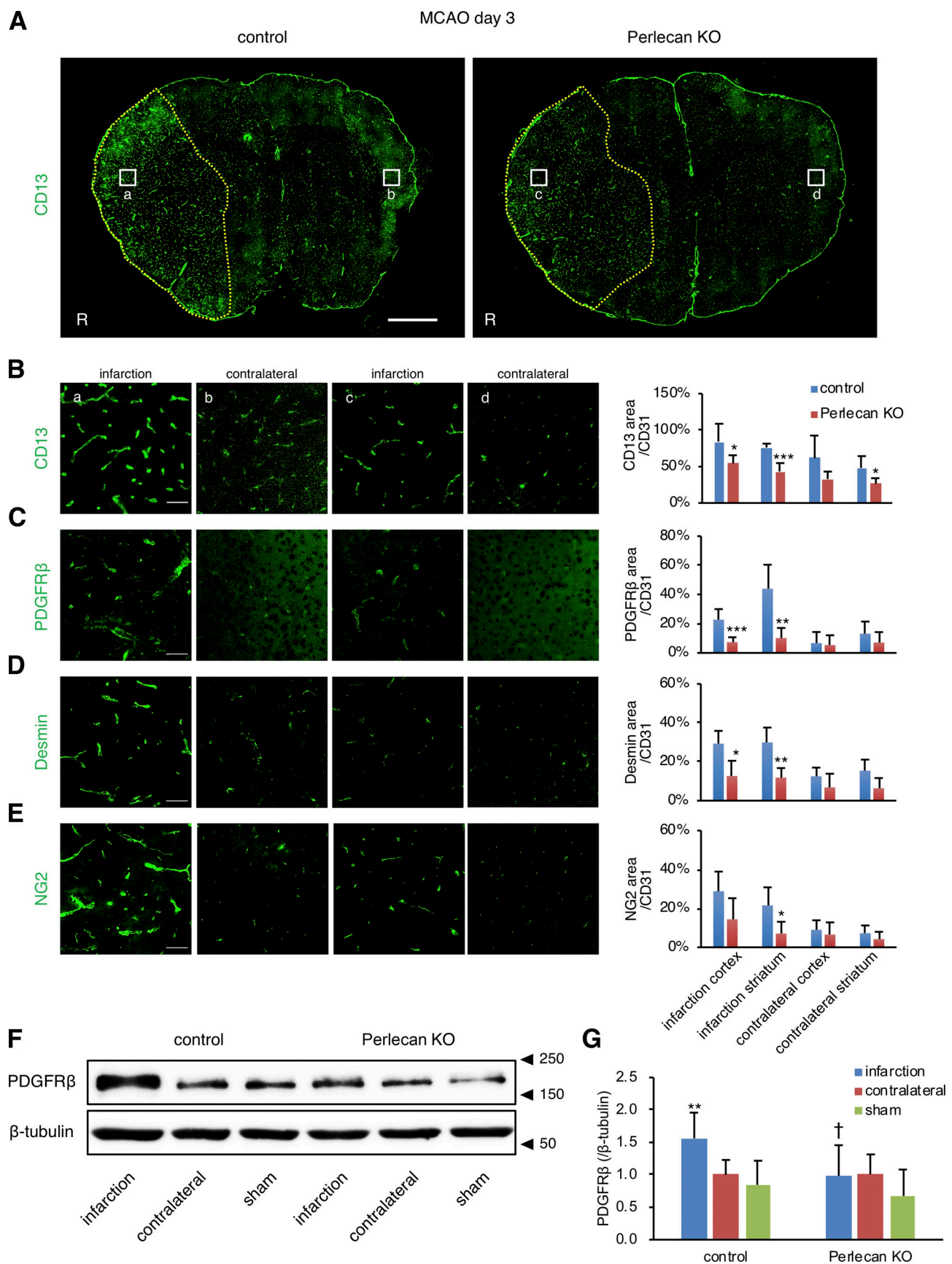


Figure 2. **The infarction-induced up-regulation of pericytes is attenuated in Perlecan KO mice.** (A) Representative images of immunostaining for the pericyte marker CD13 at PSD 3 after MCAO in control and Perlecan KO mice. The control mice showed an increase in the number of CD13<sup>+</sup> pericytes in the

ischemic lesion at PSD 3, while this up-regulation was not observed in Perlecan KO mice. Yellow dotted line = infarct area, defined by MAP2 and GFAP staining (Fig. S2 A). Scale bar = 1 mm. **(B–E)** CD13<sup>+</sup> (B), PDGFR $\beta$ <sup>+</sup> (C), desmin<sup>+</sup> (D), or NG2<sup>+</sup> (E) areas were quantified and standardized by CD31<sup>+</sup> areas in the ischemic lesions of control and Perlecan KO mice. Left panels indicate a higher magnification of the brain cortex. Scale bar = 50  $\mu$ m. Values are mean  $\pm$  SD;  $n$  = 5 mice per group; \*,  $P$  < 0.05; \*\*,  $P$  < 0.01; \*\*\*,  $P$  < 0.001 versus control mice, unpaired  $t$  test. **(F and G)** The immunoblotting for PDGFR $\beta$  in brain cortex lysates of ipsilateral or contralateral hemispheres at PSD 3 after MCAO, or sham surgery control of control and Perlecan KO mice. A representative example of five independent experiments is shown (F). Quantitative analysis by densitometry normalized with  $\beta$ -tubulin is represented as the fold increase above the expression of PDGFR $\beta$  in the contralateral hemisphere of control mice (G). Values are mean  $\pm$  SD;  $n$  = 7 mice per group or 5 (sham surgery mice); \*\*,  $P$  < 0.01 versus contralateral hemisphere; †,  $P$  < 0.05 versus control mice, one-way ANOVA followed by Dunnett's test.

of SHP-2 and FAK through PDGFR $\beta$  and integrin  $\alpha$ 5 $\beta$ 1 signaling. Moreover, FAK activation possibly facilitates the turnover of focal adhesions.

### Perlecan DV promotes PDGF-BB-induced pericyte migration

We also assessed the effect of perlecan DV on the formation of actin stress fibers and focal adhesions in pericytes following stimulation with PDGF-BB. Pericytes cultured on perlecan DV showed well-assembled stress fibers and increased numbers of focal adhesion sites compared with cells cultured without perlecan DV or PDGF-BB (Fig. 5, A–C). Moreover, colocalization of integrin  $\alpha$ 5 and focal adhesions, similar to that seen in pericytes adhering to fibronectin, was detectable in pericytes cultured on perlecan DV (Fig. S4 A). Perlecan DV and PDGF-BB stimulated colocalization of phosphorylated PDGFR $\beta$  with integrin  $\alpha$ 5 in the focal adhesions (Fig. 5, D and E). These results indicate that perlecan DV stimulates the formation of focal adhesions in pericytes through integrin  $\alpha$ 5, and that perlecan DV and PDGF-BB cooperate to induce the clustering of phospho-PDGFR $\beta$  and integrin  $\alpha$ 5.

We next examined the effect of perlecan DV on PDGF-BB-induced pericyte migration using a Boyden chemotaxis chamber (Fig. 6 A). PDGF-BB-induced pericyte migration was significantly enhanced by the perlecan DV-coated Transwell membranes (Fig. 6 B) and was inhibited by the integrin  $\alpha$ 5 blocking antibody mAb16 (Fig. 6 C). A single-cell tracking assay showed increased velocity of PDGF-BB-induced pericytes on the perlecan DV-coated plates (Fig. S4, B and C). Likewise, an in vitro wound healing assay showed that perlecan DV accelerates pericyte migration (Fig. 6, D and E), without any significant effect on pericyte proliferation (Fig. S4 D). The perlecan DV treatment did not affect the expression of PDGFR $\beta$  in cultured pericytes (Fig. S4, G and H). These results indicate that perlecan DV promotes PDGF-BB-induced pericyte migration, but not pericyte proliferation in culture.

Consistent with these in vitro observations, an in vivo BrdU incorporation assay showed no significant difference in pericyte proliferation in the infarct area of control and Perlecan KO mice at PSD 3 after MCAO (Fig. S4, E and F). We should note that there is a significant increase in pericyte proliferation in the infarct area, compared with that in the noninfarct area (Fig. S4 F, infarction versus contralateral), suggesting that the up-regulation of pericyte marker expression in the infarct area after stroke results from an increase in the number of pericytes due to enhanced pericyte proliferation and accumulation. Importantly, perlecan is involved in pericyte migration, but not proliferation.

### Administration of perlecan DV reduces the infarct size

We examined the in vivo effect of perlecan DV on ischemic stroke by intraperitoneal injection of perlecan DV for two or four consecutive days, beginning 24 h after MCAO (Fig. 7 A). The intraperitoneally injected FLAG-tagged perlecan DV was detected in the infarct area, particularly in the microvessels, by immunostaining with antibody to a 3xFLAG tag, whereas it was not detectable in the contralateral hemisphere at PSD 3 (Fig. 7 B). Perlecan DV administration increased the number of PDGFR $\beta$ -positive pericytes in the infarct area (Fig. 7, C and D). These data suggest that perlecan DV may stimulate pericyte recruitment into microvessels in the infarct area and promote BBB repair. Indeed, perlecan DV administration significantly restored the infarct area in the Perlecan KO mice at PSD 5 (Fig. 7 E), indicating a potential benefit of perlecan DV as a therapeutic agent for the treatment of ischemic stroke damage.

## Discussion

In this study, we demonstrated that perlecan, one of the major ECM components of the BBB, regulates the adhesion between the ECM and pericytes required for BBB maintenance, and it directs pericyte recruitment, a crucial process in the repair of BBB functions after ischemic stroke (Fig. 8 A). Moreover, perlecan DV enhances pericyte migration through the cooperative function of PDGFR $\beta$  and integrin  $\alpha$ 5 $\beta$ 1 signaling, thereby allowing a subsequent dynamic regulation of focal adhesions and the actin cytoskeleton (Fig. 8 B).

The ECM proteins play important roles in BBB functions. However, the mechanisms involved in BBB maintenance and repair by ECM proteins after ischemic stroke remain unclear. Laminin produced by astrocytes regulates BBB integrity and pericyte differentiation (Menezes et al., 2014; Yao et al., 2014). Fibronectin, which is produced by endothelial cells, pericytes, and astrocytes, stimulates angiogenesis and fibrosis after stroke (Li et al., 2012; Makiyama et al., 2015). Our present study suggests an involvement of perlecan in BBB repair under pathological conditions (i.e., following ischemic stroke), whereas no significant malformation or dysfunction of brain vasculature was detectable in the Perlecan KO mice under nonpathological conditions. This finding suggests that perlecan is not essential for vascular development, that BBB maturation is delayed but sufficient, or that other ECM proteins may compensate for the Perlecan deficiency during vascular development. Further experiments will be needed to reveal the developmental process of the BBB maturation in Perlecan KO mice. By contrast, the large infarct volume and the large BBB leakage observed in Perlecan KO mice may reflect a significant importance of perlecan in BBB



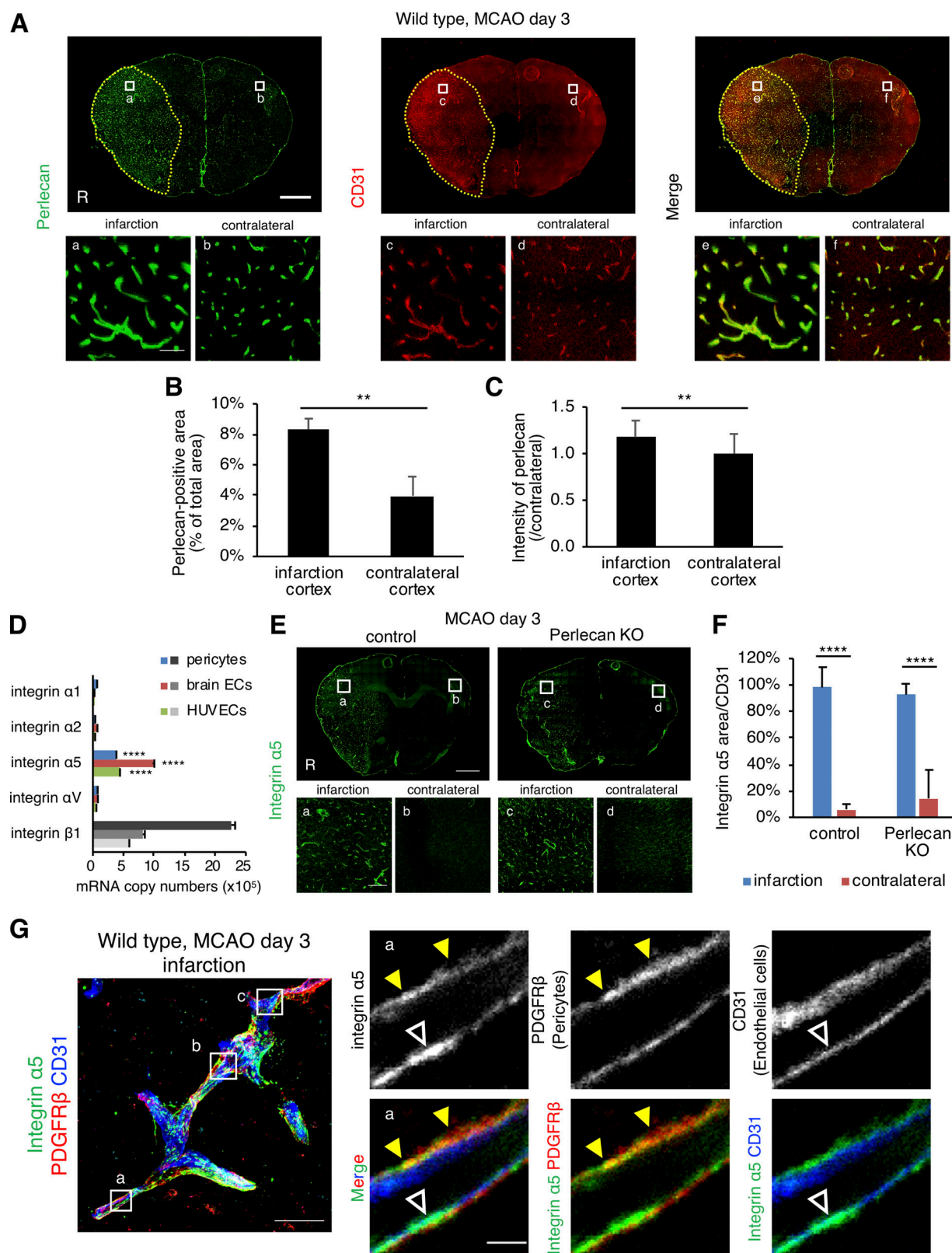


**Figure 3. The expression levels of perlecan and integrin  $\alpha 5$  are increased after ischemic stroke.** (A–C) The expression of perlecan (green) and CD31 (red) was significantly higher in the infarct areas than in the contralateral hemisphere at PSD 3 after MCAO. Scale bar = 1 mm (upper panels) or 50  $\mu$ m (lower panels). Yellow dotted line = infarct area. Perlecan-positive areas (B) and the intensity (C) were quantified in brain cortex areas of wild-type mice. Values are mean  $\pm$  SD;  $n = 5$ ; \*\*,  $P < 0.01$ , unpaired  $t$  test. (D) Quantitative real-time PCR for the expression of integrins in brain pericytes, brain endothelial cells (ECs), and human umbilical vein endothelial cells (HUVECs). Values are mean  $\pm$  SD;  $n = 3$ ; \*\*\*\*,  $P < 0.0001$  versus other integrin  $\alpha$  isoforms, one-way ANOVA followed by Tukey–Kramer’s HSD test. (E and F) The expression of integrin  $\alpha 5$  was significantly increased compared with the contralateral hemisphere at PSD 3 after

MCAO in control and Perlecan KO mice. Scale bar = 1 mm (top panel) or 100  $\mu$ m (bottom panels). Integrin  $\alpha$ 5-positive areas were quantified in brain cortex areas (F). Values are mean  $\pm$  SD;  $n = 6$  mice per group; \*\*\*\*,  $P < 0001$ , one-way ANOVA followed by Tukey–Kramer’s HSD test. **(G)** Representative images of the immunostaining for integrin  $\alpha$ 5 in brain microvessels. A maximum-intensity projection image was constructed from Z-stack images (left panel). The boxed regions in the left panel are magnified in right panels (a) and in Fig. S3 C (b and c). The expression of Integrin  $\alpha$ 5 (green) was detectable in both pericytes (PDGFR $\beta$ , red, yellow arrowheads) and endothelial cells (CD31, blue, white arrowheads). Scale bar = 20  $\mu$ m (left panel) or 2  $\mu$ m (right panels).

maintenance. Perlecan, which is distributed in the BMs between endothelial cells and pericytes, is involved in the integrity and interaction of these cells.

Many ECM proteins, including perlecan, are known to undergo degradation after ischemic stroke due to the activation of proteases, such as matrix metalloproteinases and cathepsins, with BBB breakdown as an end result (Fukuda et al., 2004; Lakhan et al., 2013). Interestingly, we found that the expression of ECM proteins, including perlecan, laminin  $\alpha$ 5, and collagen type IV, was up-regulated in the ischemic lesion in the transient

MCAO model, where vascular cells barely survive to support neovascularization. One explanation is that the up-regulation of perlecan may reflect a counteractive response during recovery from ischemic damage, so that while the BMs are degraded, the ECM composition is altered. Therefore, perlecan may be detached from BMs and activated by inflammation in the disrupted BBB after ischemic stroke. Perlecan DV, in particular, is known to be activated during BBB breakdown (Lee et al., 2011). A previous report using a brain stab wound model demonstrated that brain injury induced perlecan biosynthesis through

Table 1. Microarray analysis of hypoxia-induced gene expression in brain pericytes

Gene symbol	RefSeq ID	Protein name	Control	Hypoxia	Fold change
ITGA1	NM_181501	Integrin Subunit $\alpha$ 1	77.2	104.0	1.3
ITGA2	NM_002203	Integrin Subunit $\alpha$ 2	110.8	200.4	1.8
ITGA3	NM_002204	Integrin Subunit $\alpha$ 3	34.3	38.4	1.1
ITGA4	NM_000885	Integrin Subunit $\alpha$ 4	3.4	3.4	1.0
ITGA5	NM_002205	Integrin Subunit $\alpha$ 5	1,081.7	2,432.2	2.2 <sup>a</sup>
ITGA6	NM_000210	Integrin Subunit $\alpha$ 6	4.3	7.1	1.7
ITGA7	NM_002206	Integrin Subunit $\alpha$ 7	712.5	792.1	1.1
ITGA8	NM_003638	Integrin Subunit $\alpha$ 8	22.8	22.4	1.0
ITGA9	NM_002207	Integrin Subunit $\alpha$ 9	2.2		
ITGA10	NM_003637	Integrin Subunit $\alpha$ 10	7.8	8.2	1.0
ITGA11	NM_001004439	Integrin Subunit $\alpha$ 11	4.0	3.6	0.9
ITGAD	NM_005353	Integrin Subunit $\alpha$ D	6.2	7.3	1.2
ITGAE	NM_002208	Integrin Subunit $\alpha$ E	897.8	466.2	0.5
ITGAL	NM_002209	Integrin Subunit $\alpha$ L	9.7	11.4	1.2
ITGAM	NM_000632	Integrin Subunit $\alpha$ M	5.3	5.0	0.9
ITGAV	NM_002210	Integrin Subunit $\alpha$ V	81.2	84.3	1.0
ITGA2B	NM_000419	Integrin Subunit $\alpha$ 2b	27.1	41.8	1.5
ITGAX	NM_000887	Integrin Subunit $\alpha$ X	19.3	19.1	1.0
ITGB1	NM_133376; NM_033668	Integrin Subunit $\beta$ 1	1,692.9	2,950.6	1.7
ITGB2	NM_000211	Integrin Subunit $\beta$ 2	2.3		
ITGB3	NM_000212	Integrin Subunit $\beta$ 3	3.8	4.4	1.2
ITGB4	NM_000213; NM_001005731	Integrin Subunit $\beta$ 5	6.6	6.8	1.0
ITGB5	NM_002213	Integrin Subunit $\beta$ 5	112.5	345.2	3.1 <sup>a</sup>
ITGB6	NM_000888	Integrin Subunit $\beta$ 6	1.7		
ITGB7	NM_000889	Integrin Subunit $\beta$ 7	3.7	3.7	1.0
ITGB8	NM_002214	Integrin Subunit $\beta$ 8	1.4		

The RNA from pericytes exposed to 1% hypoxia for 24 h was labeled with Cy3 and compared with Cy5-labeled RNA of control cells. The results were analyzed in duplicate, and selected genes are listed with gene expression data as the mean value.

<sup>a</sup>Fold-change >2.



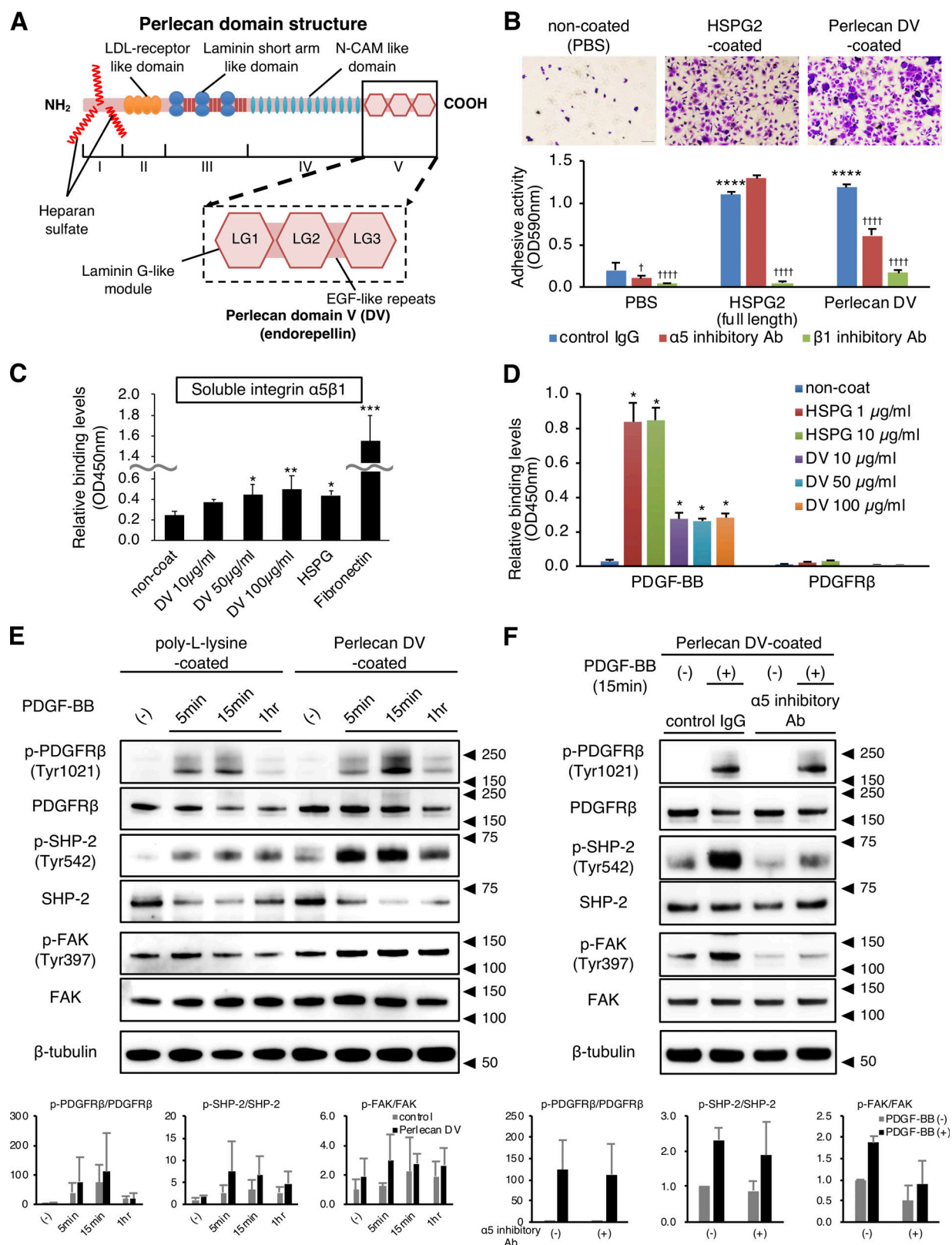


**Figure 4. Perlecan DV promotes PDGFR $\beta$  signaling through integrin  $\alpha 5 \beta 1$ .** (A) Structure of perlecan. The five domains are numbered from the N terminus to the C terminus. Domain I contains the binding sites for heparan sulfate side chains. DV/endorepellin contains three globular domains that have homology to the laminin G module (LG) and that are each separated by epidermal growth factor (EGF)-like repeats (Noonan et al., 1991; Iozzo, 2005). (B) Representative images of brain pericytes attached to immobilized full-length perlecan (HSPG2, 10  $\mu$ g/ml) or perlecan DV (500 nmol/liter; upper panels). Scale bar = 100  $\mu$ m. The adhesion of pericytes to perlecan DV was inhibited by integrin function-blocking antibodies against integrins  $\alpha 5$  (mAb16, 50 mg/ml) and  $\beta 1$  (mAb13, 50 mg/ml). Values are mean  $\pm$  SD;  $n = 5$ ; \*\*\*\*,  $P < 0.0001$  versus PBS; †,  $P < 0.05$ ; †††,  $P < 0.0001$  versus control IgG, one-way ANOVA followed by Tukey–Kramer's HSD test.

(C) Solid-phase binding assays of soluble integrin  $\alpha 5 \beta 1$  (4  $\mu\text{g/ml}$ ) to the immobilized perlecan DV (10–100  $\mu\text{g/ml}$ ), full-length perlecan (HSPG2, 10  $\mu\text{g/ml}$ ), or fibronectin (10  $\mu\text{g/ml}$ ). Values are mean  $\pm$  SD;  $n = 6$ ; \*,  $P < 0.05$ ; \*\*,  $P < 0.01$ ; \*\*\*,  $P < 0.0001$  versus noncoated, one-way ANOVA followed by Dunnett's test. (D) Solid-phase binding assays of soluble PDGF-BB (0.5  $\mu\text{g/ml}$ ) or PDGFR $\beta$  (2  $\mu\text{g/ml}$ ) to the immobilized full-length perlecan (HSPG2) or perlecan DV. Values are mean  $\pm$  SD;  $n = 3$ ; \*,  $P < 0.0001$  versus noncoated, one-way ANOVA followed by Dunnett's test. (E) The immunoblotting for the temporal profiles of p-PDGFR $\beta$  (Y1021)/PDGFR $\beta$ , p-SHP-2 (Y542)/SHP-2, and p-FAK (Y397)/FAK in pericytes. Cells were cultured on either poly-L-lysine (control, 15  $\mu\text{g/ml}$ ) or perlecan DV (500 nmol/liter). After serum starvation for 16 h, PDGF-BB (50 ng/ml) was added at the indicated time. A representative example of three independent experiments is shown (upper panels). The phosphorylated protein was quantitatively evaluated by densitometry, normalized with the total protein, and represented as the fold increase above the level obtained with control substrate without PDGF-BB (lower panels). Values are mean  $\pm$  SD;  $n = 3$ . (F) The immunoblotting for p-PDGFR $\beta$  (Y1021)/PDGFR $\beta$ , p-SHP-2 (Y542)/SHP-2, and p-FAK (Y397)/FAK in pericytes under an inhibitory antibody for integrin  $\alpha 5$ . The cells were cultured on perlecan DV, serum-starved, pretreated with either control IgG or mAb16 (50  $\mu\text{g/ml}$ ) for 1 h, and incubated with PDGF-BB (20 ng/ml) for 15 min. A representative example of three independent experiments is shown (upper panels). The data represent the fold increase above the level obtained with control IgG treatment without PDGF-BB (lower panels). Values are mean  $\pm$  SD;  $n = 3$ .

inflammatory responses (García de Yébenes et al., 1999). Further experiments should be performed to identify the mechanism underlying the up-regulation of perlecan in response to ischemic stroke.

We previously demonstrated an up-regulation of PDGFR $\beta$  following ischemic stroke. The resulting up-regulation of PDGFR $\beta$  signaling and the increased recruitment of pericytes are involved in the maintenance of the BBB (Shen et al., 2012) and in the scar formation in the infarct areas (Arimura et al., 2012; Makihara et al., 2015; Tachibana et al., 2017). PDGFR $\beta$  can essentially serve as a marker for “active pericytes,” because its expression is drastically induced in pericytes after ischemic stroke. A previous study showed that bFGF, produced by endothelial cells and pericytes, modulates the expression of PDGFR $\beta$  (Nakamura et al., 2016), but the mechanisms underlying the observed pericyte recruitment are unclear. In this study, we demonstrated that not only PDGFR $\beta$  but also other pericyte markers tested were up-regulated after ischemic stroke. Our data suggest that the up-regulation results from an increase in the number of “active pericytes” in and around the ischemic lesion and that perlecan enhances pericyte migration but not proliferation. These results suggest that perlecan not only functions as an ECM protein to support BBB integrity, but it also serves as an initiator of the BBB repair processes, including pericyte migration, after ischemic stroke.

The observed binding activity of PDGF-BB with perlecan DV suggests that endothelial cell-derived perlecan may act as a storage reservoir of PDGF-BB for pericytes to enhance PDGFR $\beta$  signaling. Perlecan deficiency may disrupt this PDGF-BB reservoir, thereby resulting in defective pericyte recruitment after ischemic stroke (Fig. 2). Indeed, perlecan is known to bind with several different growth factors and receptors, and it may prevent the diffusion of growth factors in the ECM reservoir (Mongiati et al., 2000; Matsuo and Kimura-Yoshida, 2014). Notably, perlecan interacts with bFGF and activates bFGF/FGFR signaling (Kerever et al., 2014). Likewise, perlecan may possibly enhance the activation of PDGF-BB-induced signaling through a direct association with PDGF-BB.

We initially assumed that the increase in the number of pericytes after stroke could result from a direct association of perlecan with PDGFR $\beta$  to stimulate PDGF-BB/PDGFR $\beta$  signaling, similar to the direct binding of perlecan with VEGF receptor (VEGFR) to modulate VEGF-A/VEGFR2 signaling (Goyal et al., 2011; Ishijima et al., 2012). Surprisingly, the full-length perlecan

and its C-terminus fragment DV were associated with PDGF-BB, but not with PDGFR $\beta$ . Based on previous studies that perlecan interacts with integrin  $\alpha 2 \beta 1$  (Mongiati et al., 2003; Bix et al., 2004; Woodall et al., 2008; Goyal et al., 2011) or integrin  $\alpha 5 \beta 1$  (Lee et al., 2011; Clarke et al., 2012) in endothelial cells, we hypothesized a potential involvement of integrins in pericytes. Among the different integrins, integrin  $\alpha 5 \beta 1$  was strongly expressed by brain pericytes. The expression of integrin  $\alpha 5$  was increased in pericytes in the ischemic lesion, and integrin  $\alpha 5$  was involved in the attachment of perlecan DV to pericytes. However, we cannot rule out the possibility that other isoforms of integrin  $\alpha$  subunit might be involved in the adhesion of pericytes to perlecan DV: Pericyte adhesion to perlecan DV was partially blocked by the integrin  $\alpha 5$  inhibitory antibody mAb16, but pericyte adhesion to the full-length perlecan (HSPG2) was not blocked by mAb16. Moreover, perlecan lacks the tripeptide Arg-Gly-Asp (RGD) sequence, which is a recognition sequence required for the binding of fibronectin by integrin  $\alpha 5 \beta 1$ . We could not obtain unequivocal evidence for a direct interaction between integrin  $\alpha 5 \beta 1$  and perlecan DV from the solid-phase binding assay and SPR assay. Fibronectin binds to integrin  $\alpha 5 \beta 1$  through the RGD sequence for  $\beta 1$  subunit (Mould et al., 1997), while perlecan DV, lacking the RGD sequence, may bind to integrin  $\alpha 5 \beta 1$  through an unknown binding site. The identity of the integrin  $\alpha 5 \beta 1$  binding site in both perlecan DV and full-length perlecan remains to be investigated. One potential scenario is that under resting conditions, the integrin  $\alpha 5 \beta 1$  binding site in the full length of perlecan might be hidden, while the binding site could be exposed after perlecan DV is produced by cleavage of full-length perlecan in response to pathological signals. The other scenario is that fibronectin or other molecules in the BMs may mediate the interaction with perlecan DV and integrin  $\alpha 5 \beta 1$  by forming a complex. For instance, fibrin is reported to work as a linkage protein between collagen I fibers and cells (Reyhani et al., 2014). Another report demonstrated that the binding of cells to denatured collagen II is mediated by an integrin  $\alpha 5 \beta 1$ -fibronectin bridge (Tuckwell et al., 1994). Likewise, another ECM protein, such as fibronectin, may function as a bridge between perlecan DV and integrin  $\alpha 5 \beta 1$ , even though the RGD sequence is lacking in perlecan DV. We should note that endothelial cell-specific deletion of *Integrin  $\alpha 5$*  results in an improvement of BBB integrity after stroke, indicating that endothelial integrin  $\alpha 5$  may not function as a protective role in the BBB (Roberts et al., 2017). A fully direct demonstration that

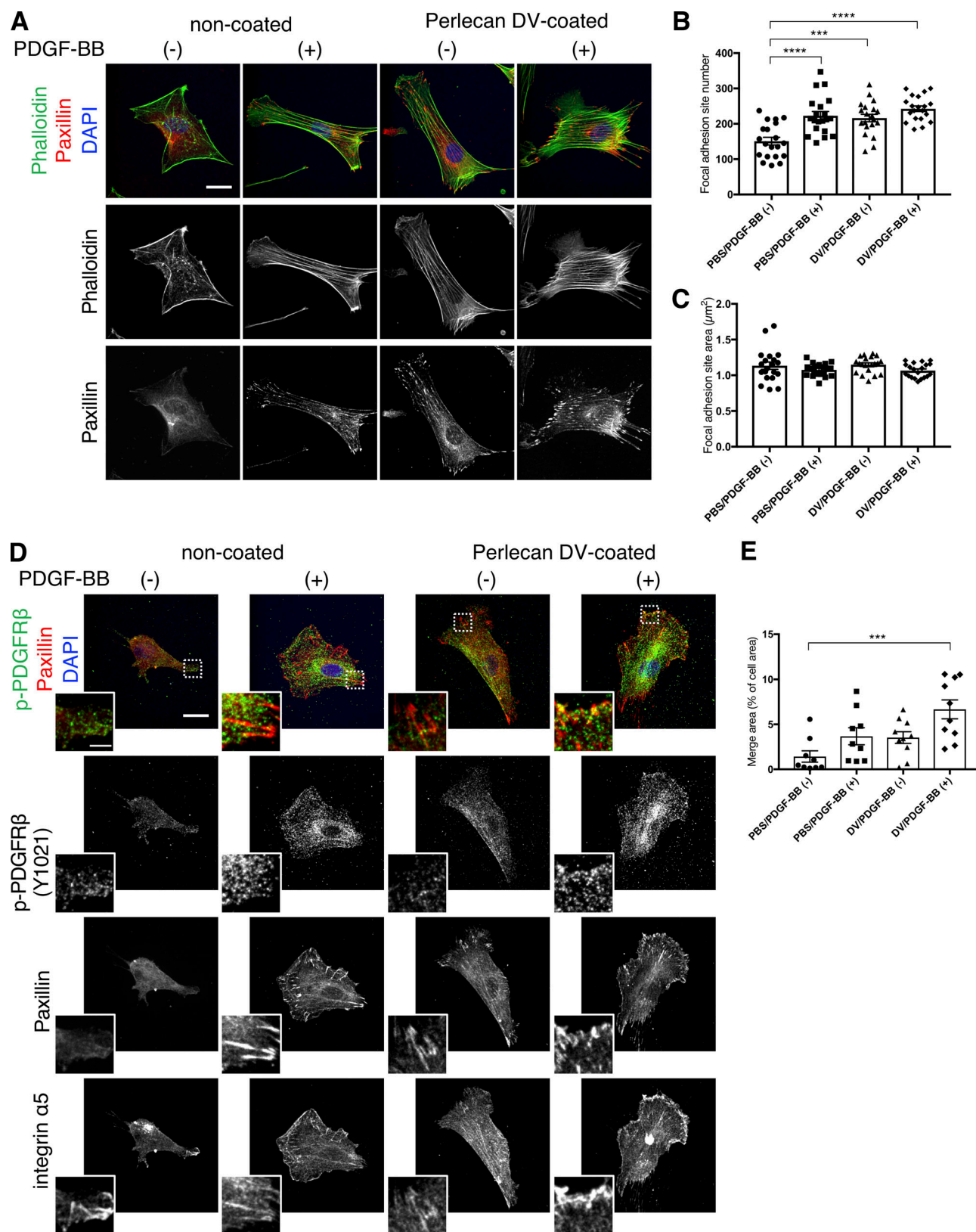


**Figure 5. Perlecan DV promotes PDGF-BB-induced actin organization and focal adhesions in pericytes.** (A) Representative images of the actin staining. Brain pericytes cultured on coverslips coated with PBS or perlecan DV (500 nmol/liter) were treated with or without PDGF-BB (50 ng/ml) for 5 min after 24-h serum starvation. Cells were stained with Alexa Fluor 488-conjugated phalloidin and anti-paxillin antibody. Scale bar = 20 μm. (B and C) The number (B) and area (C) of focal adhesion was analyzed by MetaMorph software. Values are mean ± SEM;  $n = 20$ ; \*\*\*,  $P < 0.001$ ; \*\*\*\*,  $P < 0.0001$ , one-way ANOVA followed by Tukey–Kramer’s HSD test. (D) Representative images of the immunostaining for phospho-PDGFRβ (Y1021), integrin α5, and paxillin. Brain pericytes cultured on



coverslips coated with PBS or perlecan DV (500 nmol/liter) were treated with or without PDGF-BB (50 ng/ml) for 5 min after 24-h serum starvation. Scale bar = 20  $\mu$ m. Insets indicate a higher magnification of the boxed region, scale bar = 5  $\mu$ m. **(E)** Quantification of the merged area for phospho-PDGFR $\beta$  (Y1021), integrin  $\alpha$ 5, and paxillin. The area of all colocalized particles was measured and standardized by each cell area using ImageJ. Values are mean  $\pm$  SEM;  $n = 10$ ; \*\*\*,  $P < 0.001$ , one-way ANOVA followed by Tukey–Kramer's HSD test.

perlecan enhances pericyte migration through integrin  $\alpha$ 5 after stroke will require pericyte-specific deletion of *integrin  $\alpha$ 5*.

On the one hand, perlecan DV has been reported to have an anti-angiogenic effect on endothelial cells (Mongiati et al., 2003; Bix et al., 2004; Goyal et al., 2011): perlecan DV (endorepellin) inactivates VEGFR phosphorylation in endothelial cells through the binding of perlecan DV with both VEGFR and integrin  $\alpha$ 2 $\beta$ 1 to up-regulate the phosphatase SHP-1. On the other hand, perlecan DV acts as a pro-angiogenic factor in brain endothelial cells through the binding of perlecan DV with integrin  $\alpha$ 5 $\beta$ 1 after ischemic stroke (Lee et al., 2011; Clarke et al., 2012). Our results indicate that PDGF-BB and perlecan DV cooperate to activate SHP-2 and downstream FAK in brain pericytes to enhance PEGF-BB-mediated pericyte migration. Although SHP-2 shares structural similarity with SHP-1, the two have opposite effects on downstream cascade signaling, depending on the cell type (Tamir et al., 2000; Chong and Maiese, 2007). The activation of SHP-2 in pericytes may activate FAK turnover and focal adhesions via Ras/Raf activation (Yu et al., 1998; Sweeney et al., 2016), resulting in actin reorganization during cell migration. Clustering of PDGFR $\beta$  and integrin  $\alpha$ 5 $\beta$ 1 may be required to achieve these cooperative functions. Direct cross-talk between PDGFR $\beta$  and integrin  $\alpha$ 5 $\beta$ 1, which would be consistent with the previous observation that integrin  $\alpha$ 5 $\beta$ 1-mediated PDGFR $\beta$  activation influences mesenchymal stem cell migration (Veevers-Lowe et al., 2011), may occur in the focal adhesions of pericytes to promote cell migration.

Our studies provide the possibility that perlecan DV may function as a BBB repair drug through its ability to enhance pericyte recruitment after ischemic stroke. The injected exogenous perlecan DV was detected only in and around the infarct vasculature. Probably, the disrupted BBB allowed perlecan DV to pass through the barrier. However, drug delivery efficiency to the brain following systemic injection is limited. We need to devise a way to improve drug delivery across the BBB, such as a specific peptide or a carrier with specific ligands (Rhim et al., 2013). The administration of perlecan DV reduced the infarct size in Perlecan KO mice, but it did not substantially reduce the infarction in control mice. One explanation is that the robustness of the stroke model used in this study might result in only a limited effect of perlecan DV in the control mice. In addition, perlecan DV enhances endothelial cell-derived VEGF production through integrin  $\alpha$ 5 $\beta$ 1 (Lee et al., 2011); however, VEGF can induce BBB permeability in the acute phase of ischemic stroke (Zhang et al., 2000; Jiang et al., 2014). Any preclinical trials and studies to determine the long-term effects and the clinical relevance of perlecan DV administration will require prior consideration of multiple ischemic stroke models with female and/or aged animals, different dosage forms and routes, and different time points of administration.

Taken together, our results suggest that perlecan maintains BBB integrity and regulates the recruitment of pericytes through a cooperative function of PDGFR $\beta$  and integrin  $\alpha$ 5 $\beta$ 1, thereby contributing to initiation of the repair process of the BBB as the vascular niche. Perlecan DV may therefore have potential as a therapeutic agent to treat BBB disruption following ischemic stroke.

## Materials and methods

### Animals

All mice were maintained and handled according to the animal protocol approved by the National Institute of Dental and Craniofacial Research (NIDCR) Animal Care and Use Committee (protocol number ASP 15-790). They were housed in a mouse facility affiliated with the American Association for the Accreditation of Laboratory Animal Care. *Hspg2*<sup>-/-</sup> KO (Perlecan) mice and perinatal lethality-rescued *Hspg2* KO mice (*Hspg2*<sup>-/-</sup>-TG; Perlecan<sup>-/-</sup>-TG) were generated as described previously (Arikawa-Hirasawa et al., 1999; Costell et al., 1999). The lethality-rescued Perlecan KO mice express a transgene of Perlecan under the *Col2a1* promoter and enhancer specific for cartilage. We maintained these mice in a C57BL/6 background.

### Stroke model

All animal procedures were approved by the Animal Care and Use Committee of NIDCR (ASP 15-790) and were conducted in accordance with the Animal Research: Reporting of In Vivo Experiments guidelines. We induced focal brain ischemia via the ischemia-reperfusion transient MCAO, as described previously (Shichita et al., 2009; Nakamura et al., 2016; Nishimura et al., 2016). Briefly, the mice were anesthetized with isoflurane (3% for induction and 1% for maintenance). We maintained the mouse body temperature at 36.0  $\pm$  0.3°C using a warming pad. After ligation of the right common carotid artery (CCA), a 6-0 silicon-coated monofilament suture (Doccol Corp., #602334) was inserted from the right CCA, and the right middle cerebral artery was occluded with the filament. The distance from the suture tip to the right CCA bifurcation was ~9–10 mm. 60 min after brain ischemia, we withdrew the filament to allow reperfusion of the right middle cerebral artery territory. Each postoperative mouse was carefully monitored in an individual cage with supportive care. Lidocaine hydrochloride jelly (Akorn) was topically applied to the incision site for postoperative pain relief. We subjected a total of 186 (wild-type 17, control 89, Perlecan KO 80) male mice (12.6  $\pm$  1.2 wk old, 22.7  $\pm$  3.0 g) to the stroke model. Because we aimed to reduce the variability of infarction, we subjected only male mice to this study. The following conditions excluded mice from analysis: (a) death within 24 h after MCAO ( $n = 5$ ), (b) the failure of surgery with incomplete

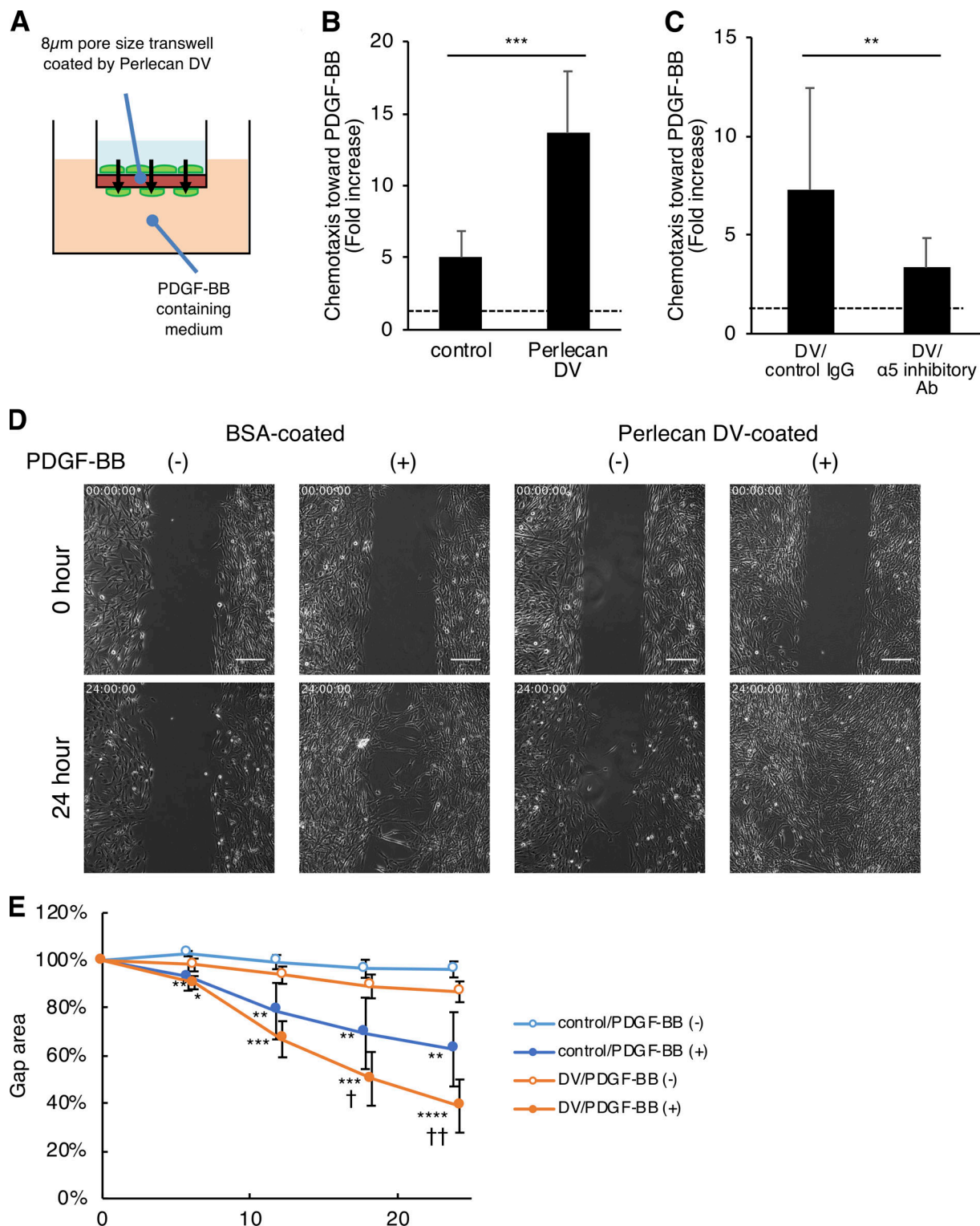


**Figure 6. Perlecan DV promotes the PDGF-BB-induced migration of pericytes.** (A and B) Brain pericytes migrating toward PDGF-BB (50 ng/ml) through a membrane coated with BSA (control) or perlecan DV (500 nmol/liter), normalized against a no-chemoattractant negative control. Values are mean  $\pm$  SD from three independent experiments conducted in triplicate; \*\*\*,  $P < 0.001$ , unpaired  $t$  test. (C) The migration of brain pericytes treated with control IgG or integrin  $\alpha$ 5 inhibitory Ab (mAb16) toward PDGF-BB (25 ng/ml) through a membrane coated with perlecan DV (500 nmol/liter), normalized against a no-chemoattractant negative control. Values are mean  $\pm$  SD from four independent experiments with triplicates; \*\*,  $P < 0.01$ , unpaired  $t$  test. (D) Brain pericytes cultured with a 500- $\mu$ m-wide gap insert on plates coated with BSA (control) or perlecan DV (500 nmol/liter) were treated with or without PDGF-BB (50 ng/ml) in serum-free medium. Representative images for the wound healing at 0 and 24 h are shown. Scale bar = 250  $\mu$ m. (E) The cell-covered area of the wound healing assay was analyzed with ImageJ and is shown as a percentage of the initial gap area. Values are mean  $\pm$  SD;  $n = 4$ –6 per group; \*,  $P < 0.05$ ; \*\*,  $P < 0.01$ ; \*\*\*,  $P < 0.001$ ; \*\*\*\*,  $P < 0.0001$  versus without PDGF-BB; †,  $P < 0.05$ ; ††,  $P < 0.01$  versus control substrate (BSA), one-way ANOVA followed by Tukey–Kramer’s HSD test.

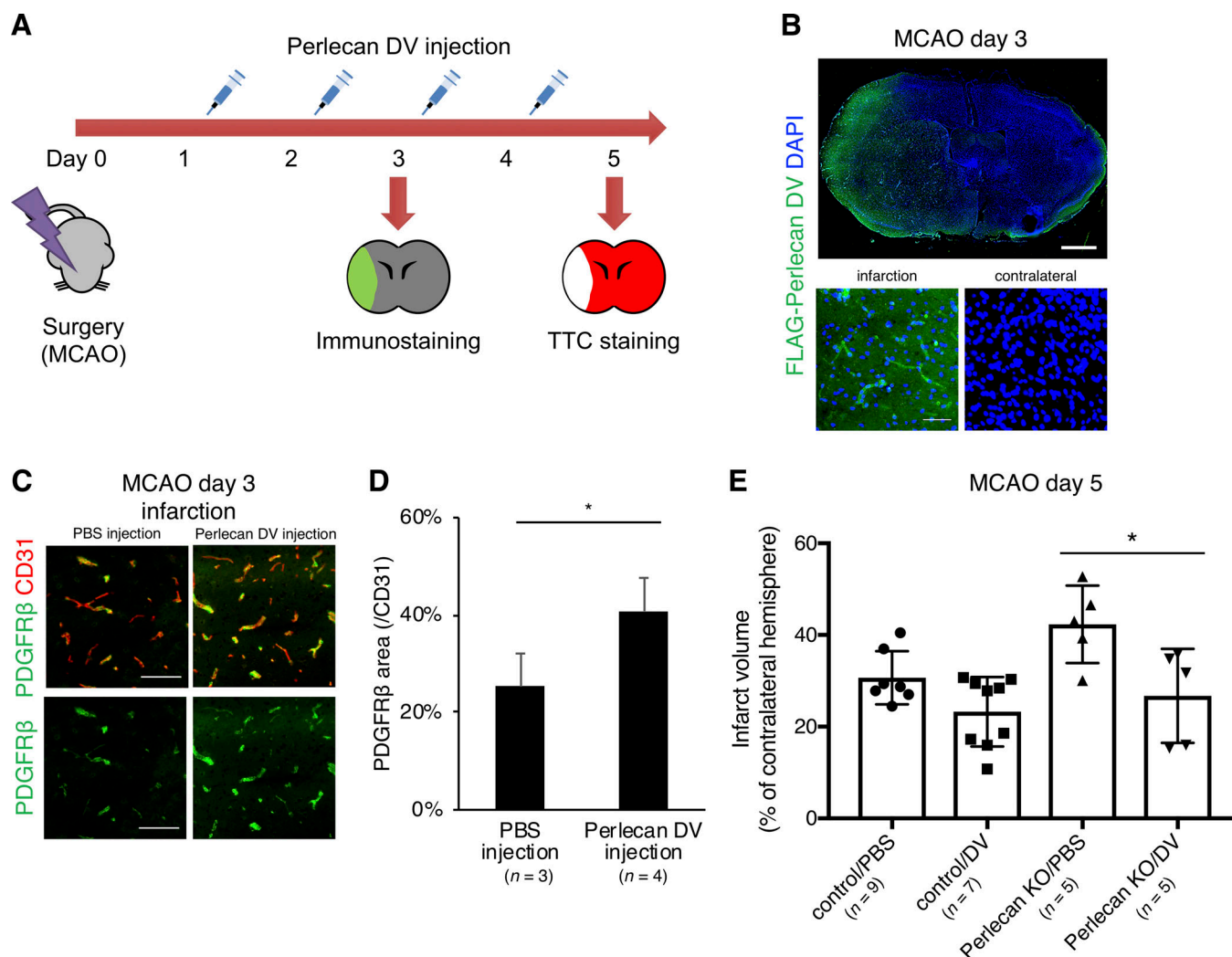


**Figure 7. Perlecan DV may promote the repair process of the BBB in ischemic stroke.** (A) Perlecan DV was intraperitoneally injected daily for two or four consecutive days starting 24 h after MCAO. The mice were sacrificed at PSD 3 after MCAO for immunostaining or at PSD 5 for TTC staining. (B) Representative images of the immunostaining for FLAG. The administered recombinant perlecan DV with 3×FLAG tag was in infarct lesion at PSD 3 after MCAO. Scale bar = 1 mm or 50  $\mu$ m. (C) Representative images of the immunostaining for PDGFR $\beta$  (green) and CD31 (red) at PSD 3 after MCAO, followed by perlecan DV injection in control mice. Perlecan DV-injected mice showed increased numbers of PDGFR $\beta$ -positive pericytes in the ischemic lesion at PSD 3. Scale bar = 100  $\mu$ m. (D) PDGFR $\beta$ -positive areas were quantified and standardized by CD31-positive areas in the brain cortex. Values are mean  $\pm$  SD; n = 3–4 per mice group; \*, P < 0.05, unpaired t test. (E) The infarction volume in Perlecan KO mice at PSD 5, evaluated by TTC staining, was significantly smaller in the mice administered perlecan DV than in mice administered PBS-vehicle. Values are mean  $\pm$  SD; n = 5–9 per mice group; \*, P < 0.05, one-way ANOVA followed by Tukey–Kramer’s HSD test.

ischemia (n = 29), (c) subarachnoid hemorrhage (n = 5), and (d) operation time >40 min (n = 2).

Physiological parameters, including blood pressure and heart rate measured by a CODA Surgical Monitor system (Kent Scientific Corp.), showed no significant differences between control and Perlecan KO mice, except for body weight (Table 2).

The effect of perlecan DV was examined by randomly treating animals with intraperitoneal injections of perlecan DV (5 mg/kg) or PBS vehicle control for two (Fig. 7, B–D) or four (Fig. 7 E) consecutive days, beginning 24 h after MCAO (Fig. 7 A).

#### Neurological deficit

Neurological sensorimotor deficits were assessed in a blinded fashion using a previously established neurological score, with modifications (0 = no observable deficit, 1 = forelimb

flexion, 2 = circling to the contralateral side, 3 = loss of walking or righting reflex, 4 = death of animal; Bederson et al., 1986; Hara et al., 1996). The survival rate after MCAO was determined by confirming the infarct area of the dead mice by TTC staining, as described below.

#### Recombinant perlecan DV production

Human Perlecan DV was cloned into the pCEP4/Pur vector containing a BM-40 signal peptide, a 6xHis tag, the cytomegalovirus promoter, and multiple cloning sites (provided by Kentaro Hozumi, Tokyo University of Pharmacy and Life Science, Tokyo, Japan; Hozumi et al., 2006) using Choo-Choo Cloning Kits (Molecular Cloning Laboratories) with the following primers: forward, 5'-GACGATAAGCTAGCGGAGATCAAGATCACC TTCCGGC-3', and reverse, 5'-CCTTGCCGGCCTCGAGCTACG



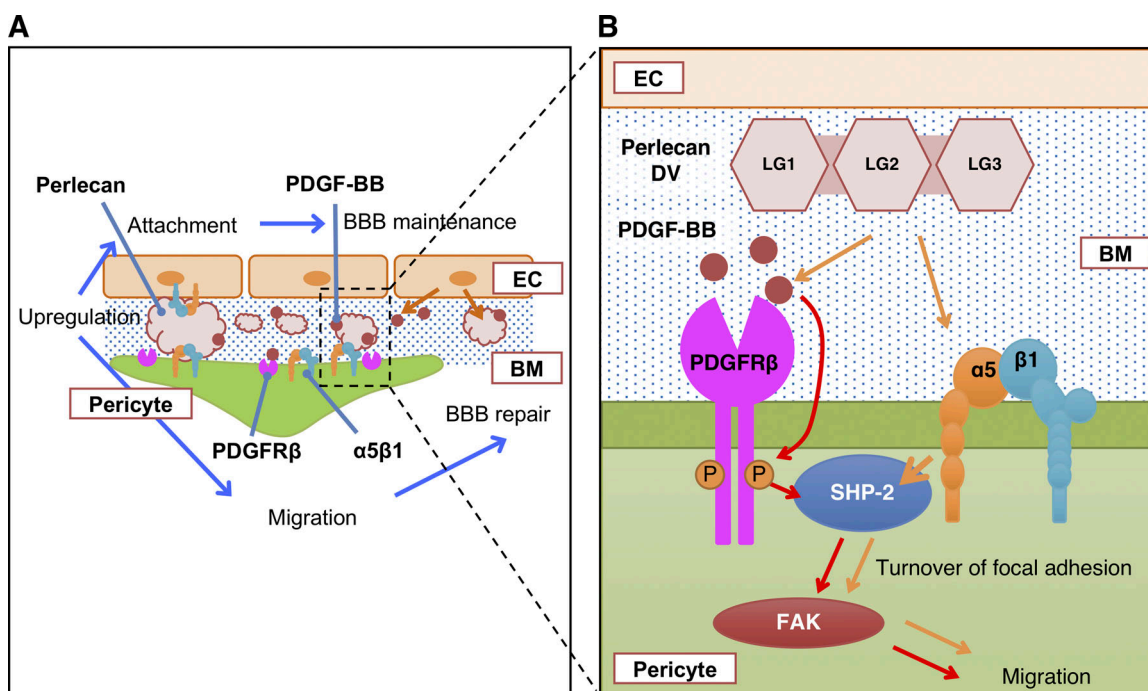


Figure 8. **Perlecan DV regulates pericyte migration through cooperative action of PDGFR $\beta$  and integrin  $\alpha 5 \beta 1$ .** Schematic model depicting the synergistic action of PDGFR $\beta$  and integrin  $\alpha 5 \beta 1$  in brain pericytes. **(A)** The up-regulated perlecan attaches to both endothelial cells (EC) and pericytes to maintain the integrity of the BBB. Perlecan interacts with pericytes to promote cell migration, thereby contributing to the repair process of the BBB. **(B)** In brain pericytes, PDGF-BB stimulation and perlecan DV synergistically induce SHP-2 phosphorylation and downstream FAK phosphorylation, causing a subsequent acceleration of focal adhesion turnover, actin reorganization, and cell migration.

AGGGGCAGGGG-3'. A plasmid containing the cDNA for human perlecan DV was a gift from Renato V. Iozzo (Thomas Jefferson University, Philadelphia, PA). The pCEP4/Pur construct was verified by DNA sequencing. The plasmid DNA was transfected into FreeStyle 293 cells (Thermo Fisher Scientific) using a 293fectin Transfection Reagent (Thermo Fisher Scientific), as described previously (de Vega et al., 2007). The cells were cultured for 72 h at 37°C in 8% CO<sub>2</sub> in a humidified incubator with rotation at 125 rpm, and the recombinant perlecan DV protein with a 6xHis tag was purified from the conditioned medium using ProBond Nickel chelating resin (Thermo Fisher Scientific), as described in the manufacturer's protocol. The recombinant protein was dialyzed overnight, and its purity was assessed by

immunoblotting (anti-6xHis Ab, Abcam, #ab18184; anti-FLAG M2-HRP conjugated Ab, Sigma-Aldrich, #A8592; Fig. S3 D). The efficiency of the *in vivo* injection of the recombinant perlecan DV protein was confirmed using DV containing a 3xFLAG tag inserted in the same vector.

#### Cell culture

Human brain pericytes and human brain endothelial cells, initiated from normal brain cortical tissues, were purchased from ScienCell Research Laboratories. Pericytes were plated on a poly-L-lysine-coated dish (Iwaki Glass) and cultured using a Pericyte Medium (ScienCell) with 2% FBS at 37°C in 5% CO<sub>2</sub> in a humidified incubator. Endothelial cells were cultured using an Endothelial Cell Medium (ScienCell) with 5% FBS. Cells were subcultured 4–10 times and then used for experiments.

#### Immunostaining

On the indicated day after MCAO, the mice were sacrificed with deep anesthesia by intraperitoneal administration of pentobarbital (75 mg/kg body weight) and perfused transcardially with ice-cold PBS and 4% PFA (Wako Chemicals USA). The brains were quickly removed and fixed with 4% PFA for 1 h. PFA-fixed coronal sections were embedded in optimal cutting temperature compound (Sakura Finetek USA) and sectioned into 14- $\mu$ m-thick slices on a cryostat (Leica Biosystems). The sections were blocked with 5% goat serum (Jackson ImmunoResearch Laboratories) and 0.3% Triton X-100 and incubated with primary antibodies overnight at 4°C, followed by the secondary antibodies

Table 2. **Physiological parameters of Perlecan KO mice.**

Characteristic	Control (n = 72)	Perlecan KO (n = 61)
Age (wk)	12.8 $\pm$ 1.0	12.6 $\pm$ 0.9
Weight (g) <sup>a</sup>	23.4 $\pm$ 2.9	21.7 $\pm$ 2.8
Ischemia time (min)	65.5 $\pm$ 4.4	65.9 $\pm$ 4.2
Systolic blood pressure (mmHg) <sup>b</sup>	131.0 $\pm$ 17.1	122.4 $\pm$ 17.0
Diastolic blood pressure (mmHg) <sup>b</sup>	89.3 $\pm$ 6.0	85.8 $\pm$ 6.0
Heart rate (/min) <sup>b</sup>	393.7 $\pm$ 63.8	385.3 $\pm$ 54.0

<sup>a</sup>P < 0.001, unpaired t test.

<sup>b</sup>n = 8 mice per group.

(Jackson ImmunoResearch Laboratories). Primary antibodies and sources were as follows: perlecan (Millipore, #MAB1948P), PDGFR $\beta$  (Cell Signaling Technology, #3169), fibrinogen (Agilent Technologies, #A0080), Claudin-5 (Thermo Fisher Scientific, #34-1600), CD31 (PECAM-1, BD Biosciences, #553370, #561813), CD13 (R&D Systems, #AF2335), desmin (Cell Signaling Technology, #5332), NG2 (Millipore, #AB5320), integrin  $\alpha$ 5 (BD Biosciences, #553350), laminin  $\alpha$ 5 (a gift from Vaishali Patel, NIDCR, Bethesda, MD), collagen type IV (Millipore, #AB769), FLAG-M2 (Sigma-Aldrich, #F3165), MAP2 (Millipore, #AB5622), and GFAP (Cell Signaling Technology, #3655). We also used DyLight 594-conjugated *Lycopersicon esculentum* (Tomato) lectin (Vector Laboratories, #FL-1177) to label vascular endothelium.

We used an A1R confocal microscope and a Slide Scanner microscope (Nikon Instruments). Nikon NIS-Elements software was used to acquire a high resolution (20 $\times$ ) tiling image. For the quantification of images, two random 600  $\times$  600- $\mu$ m fields per brain region were analyzed and averaged for each animal. The objective fluorescent signal above threshold was measured by a blinded investigator using ImageJ (National Institutes of Health).

For integrin  $\alpha$ 5 staining in mice brain sections, the sections were permeabilized by incubation in methanol for 10 min at  $-20^{\circ}\text{C}$ . Acquired Z stack images were reconstructed using the Fiji 3D Viewer plugin. For FLAG staining, the brains were extracted after the perfusion without PFA, and the sections were fixed with 1:1 acetone/methanol for 10 min at  $-20^{\circ}\text{C}$ .

Actin stress fibers and focal adhesions of cultured cells were observed after permeabilizing the cells and fixing in 1% PFA and 0.03% Triton X-100 with 10 mg/ml nonfluorescent phalloidin (Thermo Fisher Scientific) in cytoskeletal buffer (CBS; 10 mmol/liter MES, 138 mmol/liter KCl, 2 mmol/liter EGTA, 3 mmol/liter  $\text{MgCl}_2$ , and 5% sucrose, pH 6.9) at  $37^{\circ}\text{C}$ . The cells were then postfixed in 4% PFA in CBS and permeabilized with 0.5% Triton X-100 in CBS. The fixed and permeabilized cells were blocked for 1 h with 20% goat serum with M.O.M. blocking reagent (Vector Laboratories) in PHEM plus glycine buffer (60 mmol/liter Pipes, 2 mmol/liter Hepes, 10 mmol/liter EGTA, 2 mmol/liter  $\text{MgCl}_2$ , and 100 mmol/liter glycine, pH 6.9). The cells were incubated with primary antibodies (paxillin, BD Biosciences, #610051; p-PDGFR $\beta$  [Y1021], Thermo Fisher Scientific, #711359; and integrin  $\alpha$ 5 [mAb11], a gift from Kazue Matsumoto, NIDCR, Bethesda, MD) for 1 h at room temperature, followed by the secondary antibodies. We used a Spinning Disk (Yokogawa Electric Corp.) attached to an Axiovert 200M microscope (Zeiss) with a 63 $\times$  Plan-Apochromat objective (NA 1.4; Zeiss) and analyzed focal adhesions with MetaMorph imaging software (Molecular Devices).

### Infarct volume

We removed the brain on the indicated day after MCAO and sectioned it into 1-mm-thick slices that were immediately immersed in 2% TTC (Sigma-Aldrich) in 0.9% NaCl at  $37^{\circ}\text{C}$  for 10 min. Serial sections were scanned, and the areas of infarct lesions were measured using ImageJ.

### BBB leakage

The permeability of the BBB in infarct areas was assessed by the leakage of Evans Blue (Sigma-Aldrich). 6 h after the intraperitoneal

injection of 2% Evans Blue in 0.9% NaCl (10  $\mu$ l/g of body weight), the mice were perfused transcardially with ice-cold saline, and the brains were collected. We extracted the Evans Blue by immersing each brain hemisphere in 500  $\mu$ l of formamide (Sigma-Aldrich) at  $65^{\circ}\text{C}$  for 24 h and then measured the optical density of the supernatant at 620 nm.

### BrdU incorporation

We injected the mice with 1 ml of BrdU labeling reagent (Thermo Fisher Scientific) per 100 g of body weight 2 d after MCAO. The mice were sacrificed 24 h after the BrdU injection (PSD 3), and samples were prepared by the same protocol as described above. Sections were incubated in 1 N HCl for 10 min on ice and 2 N HCl for 10 min at room temperature, then 20 min at  $37^{\circ}\text{C}$  to break open the DNA structure of the labeled cells, followed by incubating the samples in borate buffer (0.1 mol/liter) for 10 min at room temperature. Then we used anti-BrdU antibody (Thermo Fisher Scientific, #B35128) with the same procedure as described above.

### Western blotting

Mouse brain samples and the cultured cells were homogenized in cell lysis buffer (Cell Signaling Technology; 20 mmol/liter Tris-HCl, pH 7.5, 150 mmol/liter NaCl, 1 mmol/liter  $\text{Na}_2\text{EDTA}$ , 1 mmol/liter EGTA, 1% Triton X-100, 2.5 mmol/liter sodium pyrophosphate, 1 mmol/liter  $\beta$ -glycerophosphate, 1 mmol/liter  $\text{Na}_3\text{VO}_4$ , 1  $\mu$ g/ml leupeptin, and protease inhibitor cocktail) at  $4^{\circ}\text{C}$  and centrifuged at 14,000  $g$  for 10 min. The protein concentration was determined using the Pierce BCA Protein Assay Kit (Thermo Fisher Scientific). The lysates, with an added sample reducing agent and electrophoresis sample buffer (Thermo Fisher Scientific), were boiled for 10 min at  $70^{\circ}\text{C}$  and subjected to 4–12% NuPAGE Bis-Tris Gel (Thermo Fisher Scientific) electrophoresis. The separated proteins were transferred to polyvinylidene fluoride membranes using an XCell Blot module (Thermo Fisher Scientific) at 30 V for 75 min. The membranes were incubated for 1 h with Block Pro (Wako) at room temperature, probed with the primary antibody overnight at  $4^{\circ}\text{C}$ , washed with 0.05% Tris-buffered saline-Tween, and incubated with the secondary antibody for 1 h at room temperature. The blots were developed using a SuperSignal West Dura Extended Duration Substrate (Thermo Fisher Scientific). Primary antibodies for PDGFR $\beta$  (#3169), p-PDGFR $\beta$  (Y1021, #227), p-SHP-2 (Y542, #3751), SHP-2 (#3752), p-FAK (Y397, #8556), FAK (#13009), and  $\beta$ -tubulin (#2128) were purchased from Cell Signaling Technology. Anti-Claudin-5 (#34-1600) and anti-ZO-1 (#40-2200) antibodies were purchased from Thermo Fisher Scientific.

### RT-PCR

Total RNAs from the cultured cells were prepared using TRIzol reagent (Thermo Fisher Scientific). Total RNA was reverse transcribed with the SuperScript IV VILO Master Mix (Thermo Fisher Scientific). Using the product as a template, PCR was performed with primers specific for the target genes (Thermo Fisher Scientific; Table S1). Quantitative real-time PCR was performed with iQ SYBR Green Supermix (Bio-Rad) using a

CFX96 Touch Real-Time PCR Detection System (Bio-Rad). The copy numbers of the mRNAs were standardized to those of *RNA18S*.

### Adhesion assays

Cell adhesion assays were performed using purified perlecan (HSPG, Sigma-Aldrich) isolated from BMs of Engelbreth-Holm-Swarm mouse sarcoma or recombinant human perlecan DV, according to a previously established method (Humphries, 2009). A 96-well cell culture plate (Corning) was coated with the adhesion molecule at 4°C overnight and blocked with 1% heat-denatured BSA at room temperature for 30 min. Cells were preincubated by rotating gently with rat IgG or rat function-blocking antibodies against integrin  $\alpha 5$  (mAb16) and  $\beta 1$  (mAb13, 50  $\mu\text{g}/\text{ml}$ ; gifts from Kazue Matsumoto) at 37°C for 1 h. A final concentration of  $3 \times 10^4$  cells/well was then spread and incubated at 37°C in 5%  $\text{CO}_2$  in an incubator for 30 min. After washing once with Dulbecco's PBS, the cells were fixed with 4% PFA and stained with 0.5% Crystal Violet (Sigma-Aldrich). The dye was extracted with 1% SDS, and the optical density at 450 nm was measured using a Cytation 5 microplate reader (BioTek U.S.).

### Solid-phase binding assays

We performed solid-phase binding assays to examine direct protein-protein binding, as described previously (Ishijima et al., 2012). A 96-well plate (Immulon 2HB flat bottom, Thermo Fisher Scientific) was coated with HSPG or perlecan DV at 4°C overnight. After blocking with 3% BSA at 37°C for 2 h, various amounts of PDGF-BB (Thermo Fisher Scientific) and PDGFR $\beta$  with the human IgG Fc portion (R&D Systems), diluted with 1% BSA, were incubated at 4°C overnight. The binding proteins were detected with anti-PDGF-BB antibody (Abcam, #ab23914) or biotinylated anti-human IgG (Thermo Fisher Scientific, #A18821), and HRP-conjugated secondary antibodies (Cell Signaling Technology) or streptavidin (Thermo Fisher Scientific). After incubation with appropriate antibodies, 3,3',5,5'-tetramethyl-benzidine (Sigma-Aldrich) solution was added to the wells and incubated for 30 min at room temperature. The colorimetric reaction of HRP was stopped by adding 2 N  $\text{H}_2\text{SO}_4$ , and the optical density at 450 nm was measured using the microplate reader.

To examine direct binding of soluble integrin  $\alpha 5\beta 1$  to immobilized perlecan DV, we coated the plate with perlecan DV, HSPG, or fibronectin (a positive control; a gift from Andrew D. Doyle, NIDCR, Bethesda, MD) at 4°C overnight. After blocking with 1% BSA in Tris-buffered saline/manganese buffer (1 mmol/liter  $\text{MnCl}_2$ , pH 7.4), the wells were incubated with 4  $\mu\text{g}/\text{ml}$  integrin  $\alpha 5\beta 1$  (R&D Systems, #3230-A5) at room temperature for 5 h. The bound integrin was fixed with 2.5% glutaraldehyde for 10 min. An integrin  $\alpha 5$ -specific antibody mAb11 was used for detection.

### SPR

SPR assays were performed with Biacore T200 (GE Healthcare). Recombinant human integrin  $\alpha 5\beta 1$  (10  $\mu\text{g}/\text{ml}$ , R&D Systems) in 10 mmol/liter sodium acetate buffer, pH 5.0, was immobilized on a CM5 sensor chip (GE Healthcare) by the amine coupling

method according to the manufacturer's protocol. The interaction of perlecan DV (0, 80, 140, 200, and 260 nM) or fibronectin (Thermo Fisher Scientific, #33016-015, 118 nM) as a positive control were measured using HBS-N buffer (GE Healthcare) with 0.05% Tween20 and 1 mmol/liter  $\text{MnCl}_2$  as running buffer at a flow rate of 30  $\mu\text{l}/\text{min}$  at 25°C. The kinetic analysis was performed using Biacore T200 evaluation software, version 2.0.

### Transwell assays

Cell migration was evaluated using polycarbonate membrane inserts (8- $\mu\text{m}$  pore size; Corning). Briefly, the membrane was coated with BSA or perlecan DV (500 nmol/liter) at 4°C overnight. A total of  $2 \times 10^5$  cells/well in serum-free medium were placed in the upper chamber after 24-h serum starvation. PDGF-BB was added to the lower chamber as a chemoattractant. After 16 h of incubation at 37°C in 5%  $\text{CO}_2$ , the migrated cells were detached from the membrane with 1 $\times$  Cell Dissociation Solution (Trevigen) and stained with calcein AM (Thermo Fisher Scientific). The fluorescence of migrated cells was measured using the microplate reader (485 nm for excitation and 520 nm for emission).

### Wound healing assays

A 12-well culture plate was coated with BSA (control) or perlecan DV (500 nmol/liter) and incubated at 4°C overnight. After washing the plate with sterilized  $\text{H}_2\text{O}$ , a silicone Culture-Insert 2 well (Ibidi) was attached; this allows the growth of cells in two separated wells with a 500- $\mu\text{m}$ -wide gap without mechanical damage due to scratching of cells and surface. A final concentration of  $2 \times 10^5$  cells/ml was applied to each well (70  $\mu\text{l}/\text{well}$ ) and incubated at 37°C in 5%  $\text{CO}_2$  for 24 h to allow cell attachment. The Culture-Insert 2 Well was then gently removed, and cells were rinsed using serum-free medium. We used an Axiovert 135TV microscope with a 10 $\times$  objective (Zeiss) to capture time-lapse images at 37°C in 5%  $\text{CO}_2$  in a humidified condition. The cell-covered area was analyzed using ImageJ.

### Proliferation assays

Cell proliferation was evaluated by the Cell Titer 96 Aqueous One Solution Cell Proliferation Assay Kit (Promega), containing the tetrazolium compound 3-(4,5-dimethylthiazol-2-yl)-5-(3-carboxymethoxyphenyl)-2-(4-sulfophenyl)-2H-tetrazolium, inner salt (MTS). A 96-well plate (Corning) was coated with poly-L-lysine (15  $\mu\text{g}/\text{ml}$ ) or perlecan DV (500 nmol/liter) at 4°C overnight. After blocking with 1% heat-denatured BSA at 37°C for 30 min, cells were seeded at  $5 \times 10^3$  cells/well and incubated as already described. At the indicated time, 20  $\mu\text{l}$  of the MTS reagent was added to each well of the assay plate (which contained the cells in 100  $\mu\text{l}$  of culture medium). The plate was then incubated for 2 h in a humidified 5%  $\text{CO}_2$  atmosphere, and the absorbance was recorded at 490 nm using a microplate reader. The background absorbance was corrected by subtracting the absorbance of a reference wavelength at 650 nm.

### Single-cell migration tracking

A glass-bottom plate (MatTek Corp.) was coated with PBS or perlecan DV (500 nmol/liter) at 4°C overnight and blocked with



1% heat-denatured BSA for 15 min. After the plate was washed three times with PBS, a total of  $4 \times 10^4$  cells/well were added. After serum starvation, nuclear staining was performed with a SiR-DNA-kit (1:1,000, Cytoskeleton), and we acquired time-lapse images for 24 h in a humidified 5% CO<sub>2</sub> atmosphere using a Zeiss Axiovert 135TV microscope. Cell tracking analysis was performed using the Fiji TrackMate plugin (Tinevez et al., 2017).

### Gene microarray analysis

Microarray analysis was performed using the 3D-Gene Human Oligo chip 25k (Toray Industries), as described previously (Nakamura et al., 2012). Total RNAs from pericytes incubated in a hypoxic chamber (1% O<sub>2</sub>) for 24 h were extracted with an RNeasy mini kit with the RNase-free DNase set (Qiagen). The Cy3- or Cy5-labeled amplified RNA samples were hybridized using the supplied protocols (<https://www.3d-gene.com>). Hybridization signals were scanned using the 3D-Gene Scanner (Toray). Microarray data were deposited in NCBI Gene Expression Omnibus and are accessible through accession no. GSE109187.

### Statistics

Statistical analyses were performed with JMP software (version 13, SAS Institute) and Prism software (version 7, GraphPad Software). We defined *n* as the number of experiments or treated animals. The statistical analysis was performed using an unpaired *t* test (two-tailed) or a one-way ANOVA. Post hoc comparisons were made using Tukey–Kramer’s honestly significant difference (HSD) test or Dunnett’s test. Data distribution was assumed to be normal, but this was not formally tested before parametric tests. A *P* value of <0.05 was considered significant.

### Online supplemental material

Fig. S1 shows the BBB morphology and tight junction proteins in Perlecan KO mice in the healthy nonstroke condition. Fig. S2 shows representative images of the immunostaining for MAP2 and GFAP and for CD13 and CD31, and neurological outcomes in Perlecan KO mice after ischemic stroke. Fig. S3 shows the immunostaining for laminin  $\alpha 5$  and collagen type IV after ischemic stroke, the immunoblot for a recombinant perlecan DV, the result from an attachment assay using brain endothelial cells with perlecan DV, and SPR assays with perlecan DV. Fig. S4 shows the colocalization of integrin  $\alpha 5$  with focal adhesion, a single-cell tracking assay using pericytes and perlecan DV, a proliferation assay, and BrdU incorporation after ischemic stroke. Table S1 shows primer pairs used in RT-PCR and quantitative real-time PCR.

### Acknowledgments

We are grateful to Dr. Kenneth M. Yamada (NIDCR, Bethesda, MD) for his critical review of the manuscript and for supplying integrin  $\alpha 5$  and  $\beta 1$  antibodies. We thank Dr. Andrew D. Doyle for his excellent technical help with microscopy observations and image analysis. We also thank Kazue Matsumoto and

Dr. Vaishali Patel for the kind gifts of antibodies, Dr. Kentaro Hozumi for the gift of pCEP4/Pur vector, and Dr. Renato V. Iozzo for the gift of human Perlecan DV (endorepellin) cDNA. We express our gratitude to Dr. Masaki Tachibana (Kyushu University) for teaching us surgical techniques and to Naoko Kasahara (Kyushu University) for the assistance with in vitro experiments. We also thank Krista Gill for editorial help and the staff at the NIDCR Veterinary Resource Core for their veterinary care of animals.

This study was supported in part by the Intramural Research Program of NIDCR, National Institutes of Health (DE000485-27 to Y. Yamada), and by the NIDCR Gene Transfer Core Facility (ZIC DE000744-04). K. Nakamura was supported by a Research Fellowship from the Uehara Memorial Foundation, a grant from SENSHIN Medical Research Foundation, and a Grant-in-Aid from the Ministry of Education, Culture, Sports, Science and Technology (19K09511). E. Arikawa-Hirasawa was supported by a Grant-in-Aid from the Ministry of Education, Culture, Sports, Science and Technology (15K09326).

The authors declare no competing financial interests.

Author contributions: K. Nakamura designed and performed experiments, analyzed the data, and wrote the manuscript. T. Ikeuchi and K. Nara assisted with in vitro experiments. C.S. Rhodes, P. Zhang, and Y. Chiba provided general technical support. S. Kazuno and Y. Miura assisted with Biacore experiments. E. Arikawa-Hirasawa created and provided the *Hspg2*<sup>-/-</sup> TG mouse line. T. Ago, Y.S. Mukouyama, and Y. Yamada designed the experiments and provided general technical support and manuscript editing. Y. Yamada directed the study.

Submitted: 24 July 2018

Revised: 10 February 2019

Accepted: 31 July 2019

### References

- Arikawa-Hirasawa, E., H. Watanabe, H. Takami, J.R. Hassell, and Y. Yamada. 1999. Perlecan is essential for cartilage and cephalic development. *Nat. Genet.* 23:354–358. <https://doi.org/10.1038/15537>
- Arimura, K., T. Ago, M. Kamouchi, K. Nakamura, K. Ishitsuka, J. Kuroda, H. Sugimori, H. Ooboshi, T. Sasaki, and T. Kitazono. 2012. PDGF receptor  $\beta$  signaling in pericytes following ischemic brain injury. *Curr. Neurovasc. Res.* 9:1–9. <https://doi.org/10.2174/156720212799297100>
- Baeten, K.M., and K. Akassoglou. 2011. Extracellular matrix and matrix receptors in blood-brain barrier formation and stroke. *Dev. Neurobiol.* 71: 1018–1039. <https://doi.org/10.1002/dneu.20954>
- Bederson, J.B., L.H. Pitts, M. Tsuji, M.C. Nishimura, R.L. Davis, and H. Bartkowski. 1986. Rat middle cerebral artery occlusion: evaluation of the model and development of a neurologic examination. *Stroke.* 17:472–476. <https://doi.org/10.1161/01.STR.17.3.472>
- Bix, G., J. Fu, E.M. Gonzalez, L. Macro, A. Barker, S. Campbell, M.M. Zutter, S.A. Santoro, J.K. Kim, M. Hook, et al. 2004. Endorepellin causes endothelial cell disassembly of actin cytoskeleton and focal adhesions through  $\alpha 2\beta 1$  integrin. *J. Cell Biol.* 166:97–109. <https://doi.org/10.1083/jcb.200401150>
- Chong, Z.Z., and K. Maiese. 2007. The Src homology 2 domain tyrosine phosphatases SHP-1 and SHP-2: diversified control of cell growth, inflammation, and injury. *Histol. Histopathol.* 22:1251–1267.
- Clarke, D.N., A. Al Ahmad, B. Lee, C. Parham, L. Auckland, A. Fertala, M. Kahle, C.S. Shaw, J. Roberts, and G.J. Bix. 2012. Perlecan Domain V induces VEGF secretion in brain endothelial cells through integrin  $\alpha 5\beta 1$  and ERK-dependent signaling pathways. *PLoS One.* 7:e45257. <https://doi.org/10.1371/journal.pone.0045257>

- Costell, M., E. Gustafsson, A. Aszódi, M. Morgelin, W. Bloch, E. Hunziker, K. Addicks, R. Timpl, and R. Fässler. 1999. Perlecan maintains the integrity of cartilage and some basement membranes. *J. Cell Biol.* 147:1109–1122. <https://doi.org/10.1083/jcb.147.5.1109>
- Del Zoppo, G.J., R. Milner, T. Mabuchi, S. Hung, X. Wang, and J.A. Koziol. 2006. Vascular matrix adhesion and the blood-brain barrier. *Biochem. Soc. Trans.* 34:1261–1266. <https://doi.org/10.1042/BST0341261>
- de Vega, S., T. Iwamoto, T. Nakamura, K. Hozumi, D.A. McKnight, L.W. Fisher, S. Fukumoto, and Y. Yamada. 2007. TM14 is a new member of the fibulin family (fibulin-7) that interacts with extracellular matrix molecules and is active for cell binding. *J. Biol. Chem.* 282:30878–30888. <https://doi.org/10.1074/jbc.M705847200>
- Fukuda, S., C.A. Fini, T. Mabuchi, J.A. Koziol, L.L. Eggleston Jr., and G.J. del Zoppo. 2004. Focal cerebral ischemia induces active proteases that degrade microvascular matrix. *Stroke*. 35:998–1004. <https://doi.org/10.1161/01.STR.0000119383.76447.05>
- García de Yébenes, E., A. Ho, T. Damani, H. Fillit, and M. Blum. 1999. Regulation of the heparan sulfate proteoglycan, perlecan, by injury and interleukin-1 $\alpha$ . *J. Neurochem.* 73:812–820. <https://doi.org/10.1046/j.1471-4159.1999.0730812.x>
- Goyal, A., N. Pal, M. Concannon, M. Paul, M. Doran, C. Poluzzi, K. Sekiguchi, J.M. Whitelock, T. Neill, and R.V. Iozzo. 2011. Endorepellin, the angiostatic module of perlecan, interacts with both the  $\alpha 2 \beta 1$  integrin and vascular endothelial growth factor receptor 2 (VEGFR2): a dual receptor antagonism. *J. Biol. Chem.* 286:25947–25962. <https://doi.org/10.1074/jbc.M111.243626>
- Hara, H., P.L. Huang, N. Panahian, M.C. Fishman, and M.A. Moskowitz. 1996. Reduced brain edema and infarction volume in mice lacking the neuronal isoform of nitric oxide synthase after transient MCA occlusion. *J. Cereb. Blood Flow Metab.* 16:605–611. <https://doi.org/10.1097/00004647-199607000-00010>
- Hellstrom, M., H. Gerhardt, M. Kalén, X. Li, U. Eriksson, H. Wolburg, and C. Betsholtz. 2001. Lack of pericytes leads to endothelial hyperplasia and abnormal vascular morphogenesis. *J. Cell Biol.* 153:543–553. <https://doi.org/10.1083/jcb.153.3.543>
- Hood, J.D., and D.A. Cheresh. 2002. Role of integrins in cell invasion and migration. *Nat. Rev. Cancer.* 2:91–100. <https://doi.org/10.1038/nrc727>
- Hozumi, K., N. Suzuki, P.K. Nielsen, M. Nomizu, and Y. Yamada. 2006. Laminin alpha chain LG4 module promotes cell attachment through syndecans and cell spreading through integrin alpha2beta1. *J. Biol. Chem.* 281:32929–32940. <https://doi.org/10.1074/jbc.M605708200>
- Humphries, M.J. 2009. Cell adhesion assays. *Methods Mol. Biol.* 522:203–210. [https://doi.org/10.1007/978-1-59745-413-1\\_14](https://doi.org/10.1007/978-1-59745-413-1_14)
- Huttenlocher, A., and A.R. Horwitz. 2011. Integrins in cell migration. *Cold Spring Harb. Perspect. Biol.* 3:a005074. <https://doi.org/10.1101/cshperspect.a005074>
- Iozzo, R.V. 2005. Basement membrane proteoglycans: from cellar to ceiling. *Nat. Rev. Mol. Cell Biol.* 6:646–656. <https://doi.org/10.1038/nrmi702>
- Ishijima, M., N. Suzuki, K. Hozumi, T. Matsunobu, K. Kosaki, H. Kaneko, J.R. Hassell, E. Arikawa-Hirasawa, and Y. Yamada. 2012. Perlecan modulates VEGF signaling and is essential for vascularization in endochondral bone formation. *Matrix Biol.* 31:234–245. <https://doi.org/10.1016/j.matbio.2012.02.006>
- Jiang, S., R. Xia, Y. Jiang, L. Wang, and F. Gao. 2014. Vascular endothelial growth factors enhance the permeability of the mouse blood-brain barrier. *PLoS One.* 9:e86407. <https://doi.org/10.1371/journal.pone.0086407>
- Kerever, A., F. Mercier, R. Nonaka, S. de Vega, Y. Oda, B. Zalc, Y. Okada, N. Hattori, Y. Yamada, and E. Arikawa-Hirasawa. 2014. Perlecan is required for FGF-2 signaling in the neural stem cell niche. *Stem Cell Res. (Amst.)*. 12:492–505. <https://doi.org/10.1016/j.scr.2013.12.009>
- Lakhan, S.E., A. Kirchgessner, D. Tepper, and A. Leonard. 2013. Matrix metalloproteinases and blood-brain barrier disruption in acute ischemic stroke. *Front. Neurol.* 4:32. <https://doi.org/10.3389/fneur.2013.00032>
- Lee, B., D. Clarke, A. Al Ahmad, M. Kahle, C. Parham, L. Auckland, C. Shaw, M. Fidanboyu, A.W. Orr, O. Ogunshola, et al. 2011. Perlecan domain V is neuroprotective and proangiogenic following ischemic stroke in rodents. *J. Clin. Invest.* 121:3005–3023. <https://doi.org/10.1172/JCI46358>
- Li, L., F. Liu, J.V. Welser-Alves, L.D. McCullough, and R. Milner. 2012. Up-regulation of fibronectin and the  $\alpha 5 \beta 1$  and  $\alpha v \beta 3$  integrins on blood vessels within the cerebral ischemic penumbra. *Exp. Neurol.* 233:283–291. <https://doi.org/10.1016/j.expneurol.2011.10.017>
- Lindahl, P., B.R. Johansson, P. Leveen, and C. Betsholtz. 1997. Pericyte loss and microaneurysm formation in PDGF-B-deficient mice. *Science*. 277:242–245. <https://doi.org/10.1126/science.277.5323.242>
- Lord, M.S., C.Y. Chuang, J. Melrose, M.J. Davies, R.V. Iozzo, and J.M. Whitelock. 2014. The role of vascular-derived perlecan in modulating cell adhesion, proliferation and growth factor signaling. *Matrix Biol.* 35:112–122. <https://doi.org/10.1016/j.matbio.2014.01.016>
- Makihara, N., K. Arimura, T. Ago, M. Tachibana, A. Nishimura, K. Nakamura, R. Matsuo, Y. Wakisaka, J. Kuroda, H. Sugimori, et al. 2015. Involvement of platelet-derived growth factor receptor  $\beta$  in fibrosis through extracellular matrix protein production after ischemic stroke. *Exp. Neurol.* 264:127–134. <https://doi.org/10.1016/j.expneurol.2014.12.007>
- Matsuo, I., and C. Kimura-Yoshida. 2014. Extracellular distribution of diffusible growth factors controlled by heparan sulfate proteoglycans during mammalian embryogenesis. *Philos. Trans. R. Soc. Lond. B Biol. Sci.* 369:20130545. <https://doi.org/10.1098/rstb.2013.0545>
- Menezes, M.J., F.K. McClenahan, C.V. Leiton, A. Aranmolate, X. Shan, and H. Colognato. 2014. The extracellular matrix protein laminin  $\alpha 2$  regulates the maturation and function of the blood-brain barrier. *J. Neurosci.* 34:15260–15280. <https://doi.org/10.1523/JNEUROSCI.3678-13.2014>
- Mongiat, M., K. Taylor, J. Otto, S. Aho, J. Uitto, J.M. Whitelock, and R.V. Iozzo. 2000. The protein core of the proteoglycan perlecan binds specifically to fibroblast growth factor-7. *J. Biol. Chem.* 275:7095–7100. <https://doi.org/10.1074/jbc.275.10.7095>
- Mongiat, M., S.M. Sweeney, J.D. San Antonio, J. Fu, and R.V. Iozzo. 2003. Endorepellin, a novel inhibitor of angiogenesis derived from the C terminus of perlecan. *J. Biol. Chem.* 278:4238–4249. <https://doi.org/10.1074/jbc.M210445200>
- Mould, A.P., J.A. Askari, S. Aota, K.M. Yamada, A. Irie, Y. Takada, H.J. Mardon, and M.J. Humphries. 1997. Defining the topology of integrin alpha5beta1-fibronectin interactions using inhibitory anti-alpha5 and anti-beta1 monoclonal antibodies. Evidence that the synergy sequence of fibronectin is recognized by the amino-terminal repeats of the alpha5 subunit. *J. Biol. Chem.* 272:17283–17292. <https://doi.org/10.1074/jbc.272.28.17283>
- Nakamura, K., M. Kamouchi, K. Arimura, A. Nishimura, J. Kuroda, K. Ishitaka, H. Tokami, H. Sugimori, T. Ago, and T. Kitazono. 2012. Extracellular acidification activates cAMP responsive element binding protein via Na<sup>+</sup>/H<sup>+</sup> exchanger isoform 1-mediated Ca<sup>2+</sup> oscillation in central nervous system pericytes. *Arterioscler. Thromb. Vasc. Biol.* 32:2670–2677. <https://doi.org/10.1161/ATVBAHA.112.254946>
- Nakamura, K., K. Arimura, A. Nishimura, M. Tachibana, Y. Yoshikawa, N. Makihara, Y. Wakisaka, J. Kuroda, M. Kamouchi, H. Ooboshi, et al. 2016. Possible involvement of basic FGF in the upregulation of PDGFR $\beta$  in pericytes after ischemic stroke. *Brain Res.* 1630:98–108. <https://doi.org/10.1016/j.brainres.2015.11.003>
- Ning, L., Z. Xu, N. Furuya, R. Nonaka, Y. Yamada, and E. Arikawa-Hirasawa. 2015. Perlecan inhibits autophagy to maintain muscle homeostasis in mouse soleus muscle. *Matrix Biol.* 48:26–35. <https://doi.org/10.1016/j.matbio.2015.08.002>
- Nishimura, A., T. Ago, J. Kuroda, K. Arimura, M. Tachibana, K. Nakamura, Y. Wakisaka, J. Sadoshima, K. Iihara, and T. Kitazono. 2016. Detrimental role of pericyte Nox4 in the acute phase of brain ischemia. *J. Cereb. Blood Flow Metab.* 36:1143–1154. <https://doi.org/10.1177/0271678X15606456>
- Nonaka, R., T. Iesaki, S. de Vega, H. Daida, T. Okada, T. Sasaki, and E. Arikawa-Hirasawa. 2015. Perlecan deficiency causes endothelial dysfunction by reducing the expression of endothelial nitric oxide synthase. *Physiol. Rep.* 3:e12272. <https://doi.org/10.14814/phy2.12272>
- Noonan, D.M., A. Fulle, P. Valente, S. Cai, E. Horigan, M. Sasaki, Y. Yamada, and J.R. Hassell. 1991. The complete sequence of perlecan, a basement membrane heparan sulfate proteoglycan, reveals extensive similarity with laminin A chain, low density lipoprotein-receptor, and the neural cell adhesion molecule. *J. Biol. Chem.* 266:22939–22947.
- Quaegebeur, A., C. Lange, and P. Carmeliet. 2011. The neurovascular link in health and disease: molecular mechanisms and therapeutic implications. *Neuron*. 71:406–424. <https://doi.org/10.1016/j.neuron.2011.07.013>
- Reyhani, V., P. Seddigh, B. Guss, R. Gustafsson, L. Rask, and K. Rubin. 2014. Fibrin binds to collagen and provides a bridge for  $\alpha v \beta 3$  integrin-dependent contraction of collagen gels. *Biochem. J.* 462:113–123. <https://doi.org/10.1042/BJ20140201>
- Rhim, T., D.Y. Lee, and M. Lee. 2013. Drug delivery systems for the treatment of ischemic stroke. *Pharm. Res.* 30:2429–2444. <https://doi.org/10.1007/s10995-012-0959-2>
- Roberts, J., L. de Hoog, and G.J. Bix. 2017. Mice deficient in endothelial  $\alpha 5$  integrin are profoundly resistant to experimental ischemic stroke. *J. Cereb. Blood Flow Metab.* 37:85–96. <https://doi.org/10.1177/0271678X15616979>

- Shen, J., Y. Ishii, G. Xu, T.C. Dang, T. Hamashima, T. Matsushima, S. Yamamoto, Y. Hattori, Y. Takatsuru, J. Nabekura, and M. Sasahara. 2012. PDGFR- $\beta$  as a positive regulator of tissue repair in a mouse model of focal cerebral ischemia. *J. Cereb. Blood Flow Metab.* 32:353–367. <https://doi.org/10.1038/jcbfm.2011.136>
- Shichita, T., Y. Sugiyama, H. Ooboshi, H. Sugimori, R. Nakagawa, I. Takada, T. Iwaki, Y. Okada, M. Iida, D.J. Cua, et al. 2009. Pivotal role of cerebral interleukin-17-producing gammadeltaT cells in the delayed phase of ischemic brain injury. *Nat. Med.* 15:946–950. <https://doi.org/10.1038/nm.1999>
- Sweeney, M.D., S. Ayyadurai, and B.V. Zlokovic. 2016. Pericytes of the neurovascular unit: key functions and signaling pathways. *Nat. Neurosci.* 19: 771–783. <https://doi.org/10.1038/nn.4288>
- Tachibana, M., T. Ago, Y. Wakisaka, J. Kuroda, M. Shijo, Y. Yoshikawa, M. Komori, A. Nishimura, N. Makihara, K. Nakamura, and T. Kitazono. 2017. Early Reperfusion After Brain Ischemia Has Beneficial Effects Beyond Rescuing Neurons. *Stroke*. 48:2222–2230. <https://doi.org/10.1161/STROKEAHA.117.016689>
- Tallquist, M.D., W.J. French, and P. Soriano. 2003. Additive effects of PDGF receptor beta signaling pathways in vascular smooth muscle cell development. *PLoS Biol.* 1:E52. <https://doi.org/10.1371/journal.pbio.0000052>
- Tamir, I., J.M. Dal Porto, and J.C. Cambier. 2000. Cytoplasmic protein tyrosine phosphatases SHP-1 and SHP-2: regulators of B cell signal transduction. *Curr. Opin. Immunol.* 12:307–315. [https://doi.org/10.1016/S0952-7915\(00\)00092-3](https://doi.org/10.1016/S0952-7915(00)00092-3)
- Tinevez, J.Y., N. Perry, J. Schindelin, G.M. Hoopes, G.D. Reynolds, E. Laplantine, S.Y. Bednarek, S.L. Shorte, and K.W. Eliceiri. 2017. TrackMate: An open and extensible platform for single-particle tracking. *Methods*. 115:80–90. <https://doi.org/10.1016/j.ymeth.2016.09.016>
- Tuckwell, D.S., S. Ayad, M.E. Grant, M. Takigawa, and M.J. Humphries. 1994. Conformation dependence of integrin-type II collagen binding. Inability of collagen peptides to support alpha 2 beta 1 binding, and mediation of adhesion to denatured collagen by a novel alpha 5 beta 1-fibronectin bridge. *J. Cell Sci.* 107:993–1005.
- Veevers-Lowe, J., S.G. Ball, A. Shuttleworth, and C.M. Kielty. 2011. Mesenchymal stem cell migration is regulated by fibronectin through  $\alpha 5 \beta 1$ -integrin-mediated activation of PDGFR- $\beta$  and potentiation of growth factor signals. *J. Cell Sci.* 124:1288–1300. <https://doi.org/10.1242/jcs.076935>
- Winkler, E.A., R.D. Bell, and B.V. Zlokovic. 2011. Central nervous system pericytes in health and disease. *Nat. Neurosci.* 14:1398–1405.
- Woodall, B.P., A. Nystrom, R.A. Iozzo, J.A. Eble, S. Niland, T. Krieg, B. Eckes, A. Pozzi, and R.V. Iozzo. 2008. Integrin  $\alpha 2 \beta 1$  is the required receptor for endorepellin angiostatic activity. *J. Biol. Chem.* 283: 2335–2343. <https://doi.org/10.1074/jbc.M708364200>
- Xu, Z., N. Ichikawa, K. Kosaki, Y. Yamada, T. Sasaki, L.Y. Sakai, H. Kurosawa, N. Hattori, and E. Arikawa-Hirasawa. 2010. Perlecan deficiency causes muscle hypertrophy, a decrease in myostatin expression, and changes in muscle fiber composition. *Matrix Biol.* 29:461–470. <https://doi.org/10.1016/j.matbio.2010.06.001>
- Yao, Y., Z.-L. Chen, E.H. Norris, and S. Strickland. 2014. Astrocytic laminin regulates pericyte differentiation and maintains blood brain barrier integrity. *Nat. Commun.* 5:3413. <https://doi.org/10.1038/ncomms4413>
- Yu, D.H., C.K. Qu, O. Henegariu, X. Lu, and G.S. Feng. 1998. Protein-tyrosine phosphatase Shp-2 regulates cell spreading, migration, and focal adhesion. *J. Biol. Chem.* 273:21125–21131. <https://doi.org/10.1074/jbc.273.33.21125>
- Zhang, Z.G., L. Zhang, Q. Jiang, R. Zhang, K. Davies, C. Powers, N. Bruggen, and M. Chopp. 2000. VEGF enhances angiogenesis and promotes blood-brain barrier leakage in the ischemic brain. *J. Clin. Invest.* 106:829–838. <https://doi.org/10.1172/JCI9369>